Final report on the project:

Nuclear Probing of Dense Plasmas

U.S. Department of Energy
Award Number:

DE-FG52-03NA00058

Recipient:

Massachusetts Institute of Technology
Cambridge, MA 02139

Principal Investigator:

Dr. Richard D. Petrasso
Plasma Science and Fusion Center
Massachusetts Institute of Technology
Cambridge, MA 02139
Tel: (617)253-8458
Fax: (617)258-7929
petrasso@psfc.mit.edu

Period covered:

15 February 2003 – 14 February 2007

Date of report:

15 May 2007

TABLE OF CONTENTS

I. EXECUTIVE SUMMARY

The object of inertial confinement fusion (ICF) is to compress a fuel capsule to a state with high enough density and temperature to ignite, starting a self-sustaining fusion burn that consumes much of the fuel and releases a large amount of energy. The national ICF research program is trying to reach this goal, especially through experiments at the OMEGA laser facility of the University of Rochester Laboratory of Laser Energetics (LLE), planned experiments at the National Ignition Facility (NIF) under construction at the Lawrence Livermore National Laboratory (LLNL), and experimental and theoretical work at other national laboratories. The work by MIT reported here has played several important roles in this national program.

First, the development of new and improved charged-particle-based plasma diagnostics has allowed the gathering of new and unique diagnostic information about the implosions of fuel capsules in ICF experiments, providing new means for evaluating experiments and for studying capsule implosion dynamics. Proton spectrometers have become the standard for evaluating the mass assembly in compressed capsules in experiments at OMEGA; the measured energy downshift of either primary or secondary D^3He fusion protons to determines the areal density, or ρR, of imploded capsules. The Proton Temporal Diagnostic measures the time history of fusion burn, and multiple proton emission imaging cameras reveal the 3-D spatial distribution of fusion burn. A new compact neutron spectrometer, for measuring fusion yield, is described here for the first time. And of especially high importance to future work is the Magnetic Recoil Spectrometer (MRS), which is a neutron spectrometer that will be used to study a range of important performance parameters in future experiments at the NIF. A prototype is currently being prepared for testing at OMEGA, using a magnet funded by this grant.

Second, MIT has used these diagnostic instruments to perform its own physics experiments and analysis with implosions at OMEGA, to provide essential data to other experimenters at LLE, and to work collaboratively with researchers from all the national laboratories (including LLNL, Los Alamos National Laboratory, and Sandia National Laboratory). Some of the implosion dynamics physics studies reported here involve the relationships between drive asymmetries and implosion asymmetries (in terms of both mass assembly and fusion burn); the time evolution of mass assembly and mass asymmetries; the behavior of shock coalescence; and the nature of fuel-shell mix.

Third, the MIT program has provided unique educational and research opportunities for both graduate and undergraduate students. The graduate students are deeply engaged in every aspect of our research program, and spend considerable time at OMEGA working on experiments and working with our collaborators from OMEGA and from the National Labs. Many undergraduates have gotten a taste of ICF research, sometimes making significant contributions. We believe that the introduction of energetic and gifted students to the challenging problems of this field and the excitement of the national lab environment leads naturally to the infusion of bright, talented young scientists into our field, and several PhD recipients from this group have become important forces in the field.

Finally, this work has provided the foundation for continuing advances during upcoming research, with other experimental and theoretical studies of implosion dynamics. In addition to the continuing application of diagnostic instrumentation used during this grant, important contributions will be made with new diagnostics such as the MRS and with new techniques based on the knowledge obtained here, such as proton radiography.

II. PROJECT ACTIVITIES AND ACCOMPLISHMENTS

The major subsections A – H below are numbered in correspondence with the major sections of the original Statement of Work, reproduced in Appendix a, while subsection I corresponds to the Statement of Work in the supplementary proposal of 2003, reproduced in Appendix b. Subsection J lists some of the activities and accomplishments that were not anticipated in the original Statements of Work. In each case, we show representative results of activities performed under the grant, and an evaluation of completeness, but the full range of work and accomplishments is more completely represented by the large number of published papers listed in Sec. IV and the conference presentations listed in Sec. V.

A. Studies of ρR, ρR symmetry, and ρR time evolution

The goals and objectives of SOW task A have all been reached, as described below.

i. Direct-drive experiments

Achieving spherical symmetry in the assembled mass of ICF capsule implosions is a critical prerequisite for optimal burn and ignition [1,2]; even in warm targets, a substantial decrease in fusion yield results from implosion asymmetries, as we will see below. Deviations from spherical symmetry can result from small-amplitude asymmetries in either initial capsule structure or laser irradiation [3,4], and it is important to have direct experimental observations of what the asymmetries look like and how they evolve. Toward that end, recent advances in charged-particle diagnostic instrumentation and analysis have made possible new measurements of implosion dynamics and symmetry. For D^3He-filled capsules, the three-dimensional spatial distribution of D^3He fusion burn can now be studied directly with proton-emission imaging (see Sec. II-B), while the time evolution of the burn can be measured with a proton temporal diagnostic (see Sec. II-F-ii). Multiple proton spectra measured at different directions can be used to determine the angular variation of capsule areal density (ρR) for D^3He- or D_2-filled capsules, and can sometimes be used to determine the time dependence of this angular variation for D^3He-filled capsules.

Absolute measurements of ρR asymmetry have now been made and studied in several contexts using proton spectrometry, through measurements of primary or secondary D^3He protons, as initially proposed by MIT, LLNL, and LLE [5]. The difference between the proton birth energy and the proton energy after transiting the capsule is a direct measure of ρR for each spectrometer line of sight. The mapping between energy loss and ρR is accomplished with our theoretical stopping-power formalism [6,7] and is relatively insensitive to uncertainties in plasma temperature, density, and composition [8]. The first definitive observation of asymmetry was made with secondary protons from D_2-filled capsules [9], while the first demonstration of the correlation between drive asymmetry and ρR asymmetry was made with D^3He-filled capsules [10]. We have since examined the relationship between drive symmetry more carefully [11] and derived and experimentally verified a scaling formula for the relationship between rms drive asymmetry amplitude and the resulting rms ρR asymmetry amplitude at compression burn time for low-mode perturbations [12]:

$$\delta\rho R_{rms}/\langle\rho R\rangle \approx 0.4(C_r\text{-}1)\ \delta I_{rms}/\langle I\rangle\ , \qquad [1]$$

where C_r is the radial convergence ratio, $\delta I_{rms}/\langle I\rangle$ is averaged over the laser pulse, and $\delta\rho R_{rms}/\langle\rho R\rangle$ is averaged over the burn interval. This scaling shows that the growth in amplitude of these low modes is dominated by Bell-Plesset-like convergence effects.

It has also been shown now [13] that Eq. [1] can be applied at individual angles and individual times during implosion, and that separate modes grow at approximately the same rate and

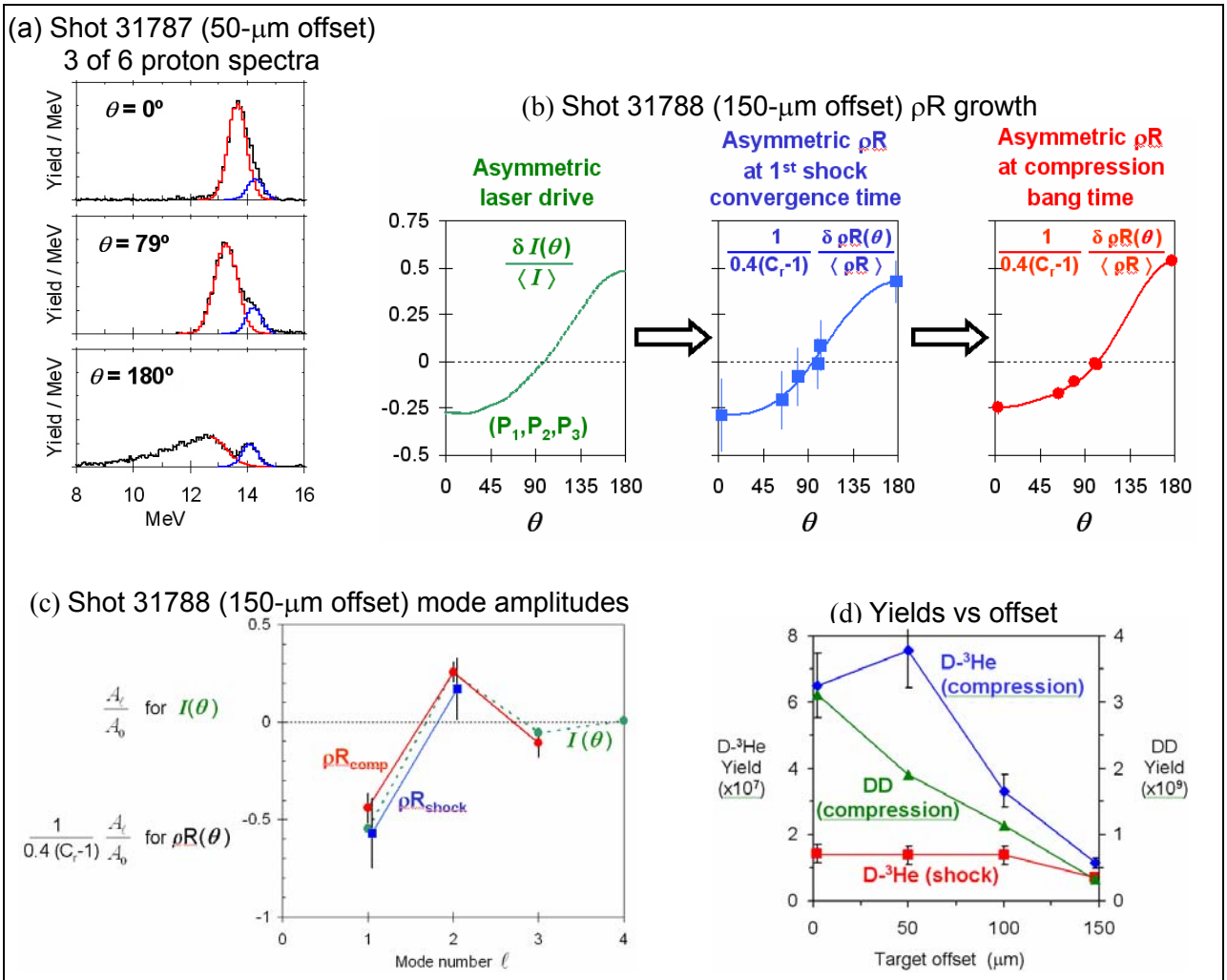

FIG. 1. Example of the how the measurement of D^3He proton spectra from different directions around an asymmetric capsule implosion at OMEGA has been used to study the effects of laser drive asymmetry on ρR asymmetry and to show how the ρR asymmetry evolves in time [14(t24)]. The laser drive asymmetry was imposed by offsetting the capsule by varying amounts from the point at which the 60 laser beams were aimed; the result was lower-than-average laser intensity on the side of the capsule facing the offset direction (θ = 0°) and higher-than-average intensity on the opposite side (θ = 180°). The data are from OMEGA shots 31787 and 31388 (capsules with 18-atm D^3He fill and a 27-μm CH shell; 23 kJ of laser energy).

(a) Three out of the six proton spectra recorded for an implosion with a 50-μm offset. Each spectrum has been decomposed into two parts, corresponding to the protons generated at the time of first shock convergence (blue) and at compression bang time (red).

(b) Angular dependence of the laser intensity compared with the angular dependence of ρR at two times. The low-mode illumination asymmetry resulted in a ρR asymmetry with the same phase, which then grew in amplitude without phase inversion. The vertical scale is the same for all three plots, and the relationship between the amplitudes of the three curves is consistent with the prediction in ref. [12] that ρR asymmetry growth should proceed primarily through effects of convergence (C_r is the radial convergence ratio). Values of ρR were inferred from the downshift of D^3He proton energies.

(c) Amplitudes of different modes in the angular structures of laser intensity and ρR for shot 31788.

(d) Yields for the DD reaction at compression and for the D^3He reaction at shock and compression times. The D^3He proton yield at shock time remains largely unaffected by the drive asymmetry caused by target offset while the yield at compression time decreases with offset

maintain their phase at least until compression burn time. Figure 1 illustrates how this was demonstrated with some of the data from a study involving varying amounts of drive asymmetry imposed by offsetting the target capsules from the location at which the laser beams are pointed resulting in deviations of the on-target laser intensity $\delta I(\phi)$ from the mean $\langle I \rangle$ that are dominated by mode numbers 1 and 2). The degradation of yield with increasing asymmetry is shown in Fig. 1d (see also Fig. 8).

The development of a new Proton Temperal Diagnostic (PTD) for measuring the time history of burn (Sec. II-F-iii) has made possible another approach to measuring the time evolution of ρR and ρR symmetry. The ρR symmetry data inherent in multiple proton spectra can be combined with direct measurements of proton production time evolution to produce a model of how the proton energy spectra are built up over time and how ρR varies with time and angular position. An example is shown in Fig. 2 [14]. In this case the ρRs grew from about 13 mg/cm^2 at shock bang time [14,15] (just before deceleration onset) to between 45 and 80 mg/cm^2 some 350 ps later at compression bang time. The ρR growth was slightly asymmetric, an occurrence that apparently depends strongly on illumination conditions [10,12].

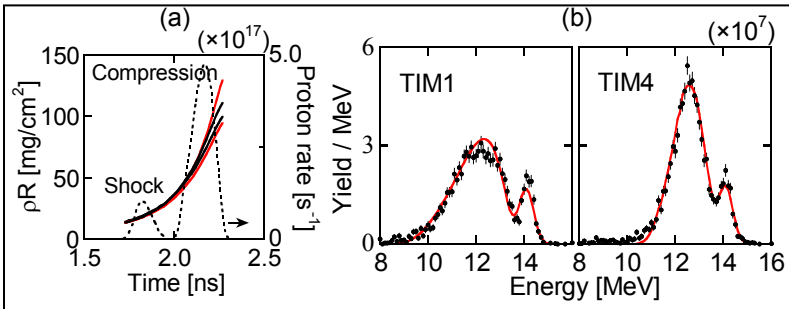

FIG. 2. The measured time evolution of ρR and ρR asymmetries (a) provides details of implosion dynamics hitherto unavailable. Evolution of ρR is inferred from the D^{3}He burn history (a) and individual proton spectra (b) from a single shot (two of six are shown) as described in Ref. [14].

The D_2 cryogenic target implosion campaign at OMEGA is a major LLE and National Program comprised of several concurrent efforts, including the experimental demonstration of improved target performance for progressively lower fuel-adiabat designs. The MIT group has worked closely with LLE scientists and has measured nuclear yields, ρR, burn-weighted asymmetries in ρR, hot-fuel ρR, and ρR evolution, and then collaborated to compare the results to simulations. Figure 3 provides an illustration of this effort; Fig. 3a shows a 2-D simulation for density contours near peak burn, and Fig. 3b compares the range of predicted and measured ρR at different angles [16].

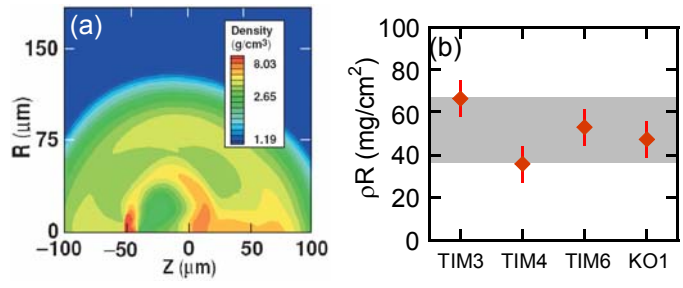

FIG. 3. Measured ρR and ρR asymmetries for a cryogenic D_2 implosion provide a stringent test of 2-D simulations. (a) 2-D DRACO simulation of the density near peak burn (shot 33600) [16]. (b) Comparison of measured ρR values at four angles (data points from different OMEGA ports) to predicted range of ρR values (gray band).

As another example, Fig. 4a illustrates the first measurement of ρR evolution in a cryogenic D_2 implosion [17]. This result was obtained by combining measured secondary proton spectra (Fig. 4b) with the DD burn history (Fig. 4 a). Also notable in Fig. 4 is the absence of any pronounced shock component in the DD burn history. As discussed earlier, measuring shock bang timing is important for determining the drive efficiency.

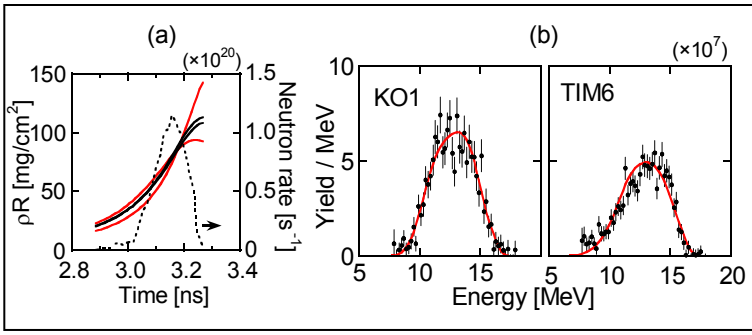

FIG. 4. The measured time evolution of ρR and ρR asymmetries provides details of D_2 cryogenic implosion dynamics hitherto unavailable (shot 35713). These results are inferred from the DD burn history [dashed line in (a)] and proton spectra from different directions (b) [14].

Most of the results shown above are for ℓ=1 drive asymmetries. Measurements of ρR asymmetries were also made during experiments with ℓ=2 drive asymmetries that were set up primarily for studying burn asymmetries using proton emission imaging cameras (Secs. II-B, II-F-ii). In those cases, detailed comparisons were made between the drive asymmetry, fusion burn asymmetry, x-ray image asymmetry, and ρR asymmetry. It was found that x-ray images, which were primarily sensitive to radiation from the hot shell near the fuel-shell interface, mirrored perfectly the asymmetries seen in the burn distributions (see Fig. 8), while very little ρR asymmetry was measured except when the burn asymmetry was very large (as in Fig. 7). The tentative conclusion is that for modest ℓ = 1 implosion asymmetry amplitudes there must be enough lateral mass flow in the shell to largely equalize ρR. This is a subject undergoing further study.

Other studies of the behavior of ρR at shock-convergence time are discussed in Sec. II-E, and other applications of the PTD are discussed in Sec. II-F-ii.

ii. Indirect-drive experiments

With indirect drive [1,2,18] being the focus of the first NIF ignition experiments in 2010, LLNL scientists Drs. P. Amendt, N. Izumi, J. Koch, and O. Landen have collaborated with MIT, conducting several indirect drive campaigns at OMEGA with the aim of clarifying different physics issues and benchmarking simulations. Our contribution to this collaboration is through the measurement and interpretation of ρR and ρR asymmetries, nuclear reaction yields, T_i, and drive efficiency. To explore capsule implosions with high-radiation-temperature drive, a series of experiments was conducted with OMEGA scale-3/4 Au and cocktail hohlraums and a NIF-like case-to-capsule ratio. Figure 5a shows a schematic of the experiment and the comprehensive set of diagnostics deployed. 2-D simulations [19] predicted, under the assumption of low laser-plasma-interaction (LPI) effects, that there should be separate and distinct features corresponding to shock and compression in proton spectra [19,20]. However, Fig. 3b shows three measurements indicating that distinct shock and compression peaks do not exist in the measured spectra of D^3He protons (as they do in direct-drive data such as those shown in Figs. 1a and 13b). For other implosions in this campaign, the predictions (again for the assumption of low LPI) indicated that the shock yield should significantly exceed the compression yield (see Fig. 5c). However, this was not observed in the experiments [19,20]. LLNL has presented the preliminary results in APS2004. More experiments have been planned by LLNL for extending this campaign.

Experiments were also performed with different laser pointing and different capsule fill pressures, on the expectation of detecting ℓ=2 ρR asymmetries, but no such asymmetries were seen in the proton data.

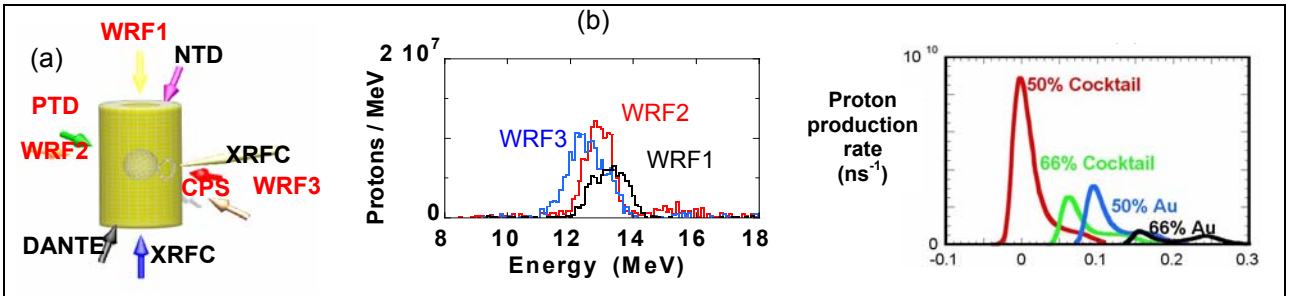

FIG. 5. (a) For various hohlraum compositions and laser-entrance holes (LEH), ρR diagnostics (WRF1-3) provided important insights into implosions. (b) For a D^3He implosion, three spectra were obtained; contrary to simulations, none show distinct shock and compression components. (c) Simulations for all hohlraums in this campaign predicted a strong shock component [the data in (b) correspond to the "66%-Au" case; the percentage refers to the LEH size]. For these scale 3/4 hohlraums, enhanced LPI is thought to be the source of the discrepancy (see text).

B. Proton-emission imaging studies of spatial burn distributions

Measured burn images and burn profiles provide compelling insight into implosion dynamics, including the combined effects of mix, hydro efficiency, and electron and radiation transport. To that end, we developed a method of imaging with D^3He protons produced in implosions of capsules filled with D^3He fuel, using multiple imaging cameras from up to three directions simultaneously for quantitative, 3-D spatial measurements of the fusion burn region in direct-drive implosions on OMEGA. Images from three orthogonal penumbral imaging cameras are processed with special algorithms [21-23] to find either the radial profile of D^3He reactions per unit volume, when burn is spherically symmetric, or the surface brightness of burn regions with arbitrary asymmetric structure. Information about the hardware is discussed in Sec. II-F-ii; here we show some experimental results. The goals and objectives of SOW task B have all been reached.

i. Radial burn-region profiles and sizes of different implosion types

Figure 6a shows a sample radial profile of burn for a symmetric OMEGA implosion, while Fig. 6b shows examples of how the size of the burn region varies for different laser energies and shell types. The burn regions of imploded thin-glass-shell capsules get larger with increasing laser energies; the burn regions of thick-plastic-shell capsules are, not surprisingly, significantly smaller than those of glass-shell capsules imploded with the same laser energy. Figure 6c shows that decreasing fill pressure can lead to diminished burn region size, even though shell convergence (as indicated by ρR) does not notably increase. This is supported by our previous finding [24] from studies of similar DT implosions that a reduction of pressure did not lead to much increase in radial convergence, in contrast to predictions of 1D codes, and was probably an indication of increased fuel-shell mix; the reduction in burn region size at lower pressures seen here may be another sign that mix is more extensive, cooling more of the outer fuel region.

ii. 3-D burn asymmetries resulting from drive asymmetry and capsule asymmetry

Figure 7 shows an example of how (intentionally) asymmetric laser drive results in an asymmetric burn region. Similar results for different types and amplitudes of drive asymmetry, and for capsule shell asymmetry, show clear correlations between drive and capsule conditions and burn asymmetry. Spatial distributions of drive, capsule shell thickness, and burn will be represented here as sums of Legendre polynomials $\sum_\ell A_\ell P_\ell(\cos\theta)$. We are interested here in low mode numbers, and will talk primarily about P_2 asymmetries that are quantified by the ratio A_2/A_0. The effects of drive asymmetry on spherical capsules were studied in a series of experiments using 17-μm-thick CH shells, with 860-μm outer

diameters, filled with 20 atm of D^3He. The laser drive was provided by OMEGA's 60 beams in a 1-ns square, 18 kJ pulse, but the intensities of individual beams were adjusted to produce nearly pure P_2 distortions with several values of the ratio $(A_2/A_0)_{drive}$ spanning the range from -0.36 to +0.17. For each case, the ratio $(A_2/A_0)_{drive}$ describing the burn distribution was determined from the imaging data. The images shown in Fig. 7 were recorded from the direction of a pole and from two nearly orthogonal directions for the case $(A_2/A_0)_{drive} = -0.36$; they show that the burn region was elongated precisely along the symmetry axis,

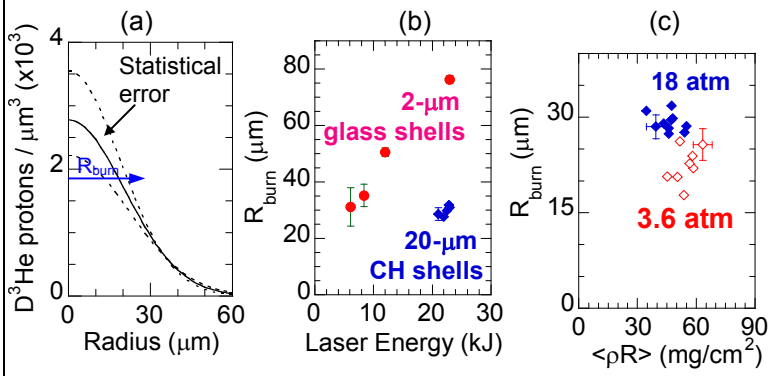

FIG. 6. Measurements of burn region size show the effects of different drive and capsule parameters for symmetric OMEGA implosions [22]. (a) Sample radial profile of D^3He emissivity is approximately Gaussian, with a burn radius R_{burn} defined at the 1/e point. (b) R_{burn} *vs.* on-target laser energy for glass and CH shells. (c) R_{burn} *vs.* ρR for imploded capsules with 20-μm CH shells and different fill pressures. The smaller burn region for the lower pressure is related to compression and mix, as discussed in the text.

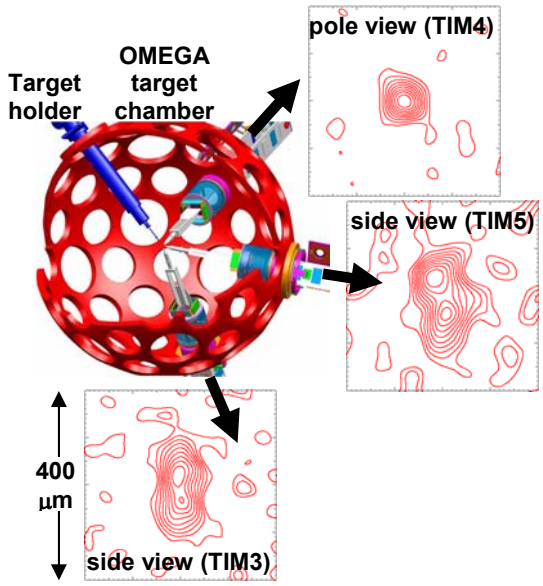

FIG. 7. 3-D imaging of D^3He burn shows the effects of drive asymmetry on implosions at OMEGA. The contour plots show surface brightness of the burn region as seen simultaneously from three orthogonal directions by separate proton emission cameras [21,25]. Prolate burn asymmetry resulted from (intentional) laser drive asymmetry with lower than average illumination in two opposing directions. The pole view is along the axis of symmetry, both side views are orthogonal to it. Burn images are important, as they reflect the cumulative effects of drive, compression, and mix. The images shown represent OMEGA shots 35172 and35173 (summed to improve statistics).

The effect of low-mode variations in capsule shell thickness was studied in a separate experiment using 860-μm diameter, 20-μm-thick CH shells, filled with 18 atm of D^3He, and symmetric drive in a 1-ns-square, 22 kJ pulse. A symmetric capsule was used for reference, and proton-emission images of the spatial distributions of D^3He reactions indicated spherical symmetry. To see the effects of shimming, we used a capsule that was essentially identical except that the shell thickness was 19.1 μm at the equator and 21 μm at the pole $[(A_2/A_0)_{shell} = 0.07]$. Some results of that experiment are shown in Fig. 8. The proton-emission images indicate that the spatial distribution of fusion reactions was prolate, with symmetry axis aligned with that of the shimmed target capsule; there was less compression of the hot fuel where the shell was thicker. This was precisely the effect expected, and was repeated in a second experiment. In addition to proton-emission images, x-ray images were recorded at bang time. The image shown in Fig. 8 demonstrates that the inner shell surface was also prolate, with the same axis of symmetry as the emission image and a slightly larger size.

The asymmetries of all the burn regions in these experiments can be quantified by measuring $(A_2/A_0)_{burn}$ from the images [23]; these are plotted in Fig. 9. Figure 10 shows both the D^3He and DD yields. Although the two series of experiments utilized slightly different capsule and drive conditions, as discussed above, they were quite similar and allow us to do some general comparisons. From Figs. 9 and 10, it can be seen that relatively small deviations of either drive or shell thickness from spherical symmetry leads to significant falloff of fusion yields in conjunction with a loss of burn symmetry.

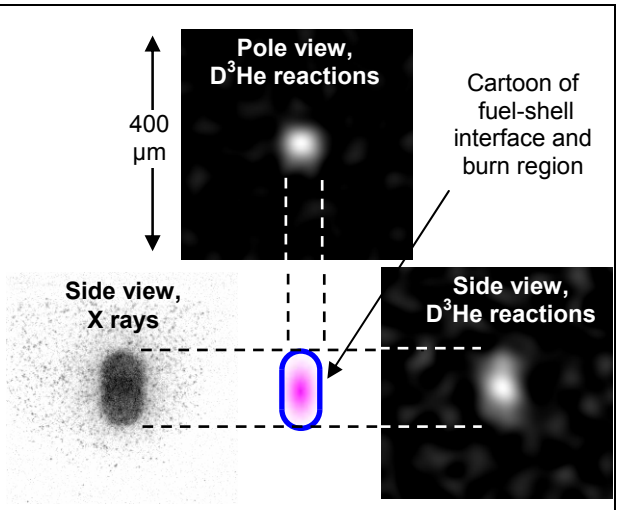

FIG. 8. Images of the spatial distribution of D^3He reactions in the compressed fuel (top and right), and the spatial distribution of 4–5 keV x-rays from the fuel-shell interface (left), at bangtime for OMEGA shot 40532 utilizing the shimmed target.

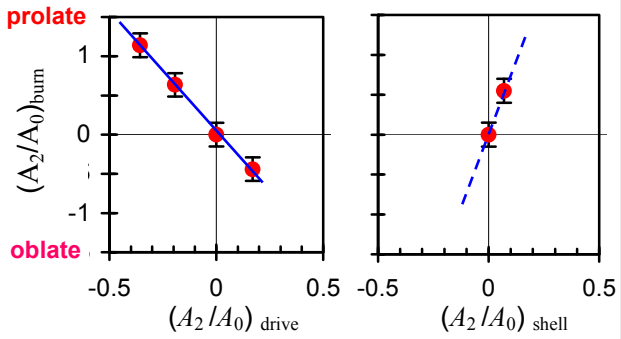

FIG. 9. Measured dependence of nuclear burn asymmetry on drive asymmetry for spherical capsules (left) and on shell-thickness asymmetry for spherical drive (right). The mean shell thicknesses, D^3He fill pressures, and total laser power were slightly different for the two sets of experiments, as described in the text, but were similar.

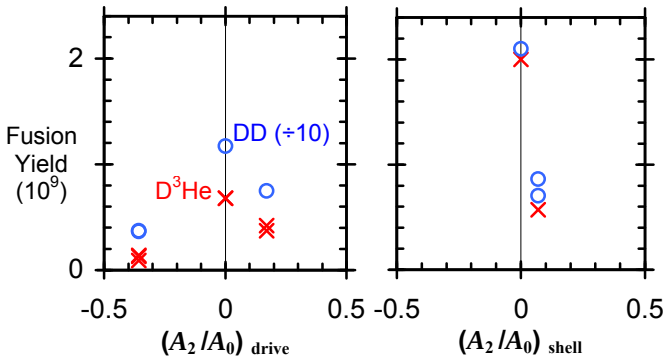

FIG. 10. Measured dependence of fusion yield on drive asymmetry (left) and on shell asymmetry (right), showing that all yields decrease quickly as the burn region loses spherical symmetry. Red Xs represent D^3He yields, and blue circles represent DD yields (shown at 1/10 their actual values).

From Fig. 9, it can be seen that both drive asymmetry and shell asymmetry lead to burn asymmetry in systematic and expected ways. This implies that it should be possible to compensate for drive asymmetry with an appropriate amount of intentional shell asymmetry (shell "shimming" [26]). From the slopes of the two plots, which differ by a factor of about -2.5, we might predict that implosion symmetry would be approximately maintained if $(A_2/A_0)_{shell} \approx 0.4\ (A_2/A_0)_{drive}$. We have shown that the trends seen in Fig. 9 are understandable as logical consequences of the "rocket equation" description of shell acceleration due to radiation-induced shell ablation [1], and that an analytic model [23] can be used to predict the amount of shell shimming that would result in greatly reduced implosion asymmetry in situations where drive asymmetry is unavoidable (such as "polar direct drive" [27] in anticipated experiments at the National Ignition Facility).

C. The slowing down of charged particles in dense plasmas

Stopping power experiments require a particle source, a particle detector with energy discrimination, and a well-characterized plasma through which to pass the particles. We have developed several high-accuracy technologies for detecting individual charged particles and measuring their energies, as described in Sec. II-F and Ref. [8]. We have also developed backlighter sources of charged particles, demonstrated by our recent and successful work doing monoenergetic proton radiography of laser-plasma interactions and capsule implosions using 14.7-MeV protons from implosions of D^3He-filled capsules [28-31]. We have started to expand the functionality of the monoenergetic backlighter sources, and to extend and apply this technique to a wider class of plasma and basic physics experiments. Furthermore, we have started to explore different venues in which other workers might benefit from the use of the unique properties of the monoenergetic particle backlighters and their associated detector technology.

First, to expand the functionality of the backlighter sources, we will develop the capability of using two or three 14.7-MeV backlighters simultaneously. This will allow different views to be obtained on a single experiment, or, alternatively, different times over a several ns period. (Each monoenergetic source, the result of the nuclear burn of a D^3He-filled exploding pusher, gates "on" for 150 ps.) In addition, we will develop particle backlighting with 9.5-MeV deuterons (D) from one branch (43%) of T^3He reactions:

$$T + {}^3He \rightarrow \alpha\ (4.8\ MeV) + D\ (9.5\ MeV)\ . \qquad (8)$$

Figure 11 shows a spectrum of these particles measured with our spectrometers during an implosion at OMEGA.

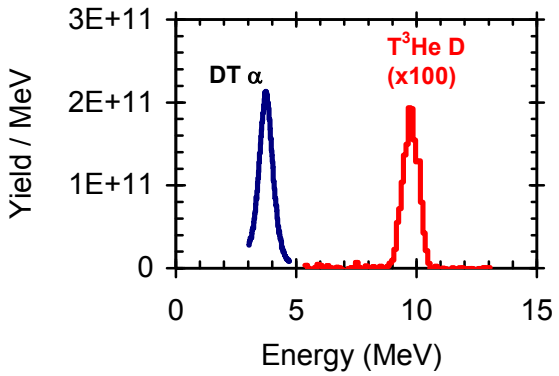

FIG. 11. Spectra of both alphas and deuterons from a non-optimized, 60-beam OMEGA imploded-pusher implosion. With very different plasma stopping power and gyro radii, these two particles complement the 14.7-MeV proton by adding new information about both fields and areal density. In particular, the 9.5-MeV deuterons have a penetration and magnetic deflection that is distinctly different (and smaller) than the 14.7-MeV proton.

Second, to extend this technique to HED physics experiments in which precise, time-resolved field measurements are a necessity, and experiments involving strongly coupled, Warm Dense Matter (WDM) where the energy loss of monoeneregetic, charged particles can be related to the dynamic interaction between the transiting particles and the WDM.

Third, to explore the feasibility of using such particles to investigate the predictions of different stopping models for well characterized plasmas, whether classical, degenerate, and/or strongly coupled.

Thus we have succeeded in developing two of the three elements required for stopping power experiments, and we are actively working on developing a means for generating a well-characterized plasma. This task is therefore ongoing.

D. Fuel-shell mix in capsule implosions

i. Direct-drive experiments

Ignition and high gain in ICF are critically dependent on mitigation of the Rayleigh-Taylor (RT) instability. The RT instability, which is the growth of nonuniformities at a density interface when a low-density material accelerates a high-density material, occurs during two distinct intervals in ICF implosions. During the acceleration phase, the low-density ablating plasma accelerates the solid shell inwards, and perturbations seeded by energy deposition nonuniformities or initial capsule surface roughness feeds through to the inner fuel-shell surface. During the deceleration phase, shortly before the time of maximum capsule compression, growth of the RT instability at the fuel-shell interface quickly saturates, resulting in small-scale, turbulent eddies that leads to atomic-scale mixing of the fuel and shell. RT growth and the resulting mixing processes disrupt the formation of the hot-spot in the fuel, lowering its temperature and reducing its volume, which may prevent the capsule from igniting. Understanding the nature and timing of RT growth and mix under different conditions is an important step toward mitigating their adverse effects.

To this end, the first temporal measurements of D^3He protons emitted from ICF implosions of CD-shelled, ^3He-filled capsules offer new and valuable insights into the dynamics of turbulent mixing induced by saturation of the Rayleigh-Taylor instability [32]. These measurements have demonstrated that bang time is substantially delayed as RT growth saturates to produce mix (Fig. 12). The 75±30 ps bang time delay of CD implosions compared to D^3He-filled, CH implosions for high initial fill densities is equal to half the burn duration. Reducing ρ_0 by a factor of five increases the susceptibility of the implosion to mix [33], and does not significantly affect the bang time delay. Continued mixing of the fill gas and shell prolongs nuclear production in CD capsules even after it is quenched in equivalent CH capsules. Finally, the relatively small increase in areal density ρL measured in CD compared to CH capsules, despite the later bang time, suggests that nuclear production is dominated by mixing induced at the tips of RT spikes driven into the core.

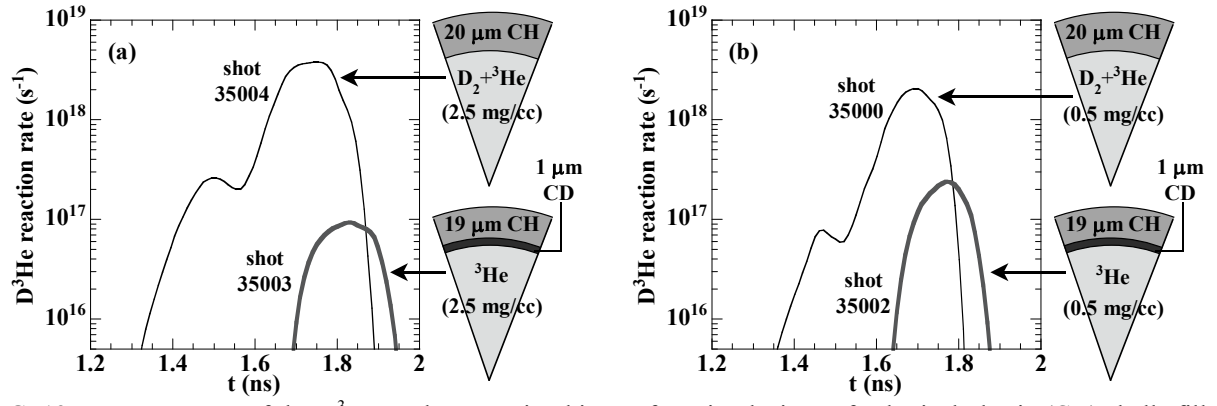

FIG. 12: Measurements of the D^3He nuclear reaction history from implosions of spherical plastic (CH) shells filled with an equimolar D_2-^3He mixture, and of equivalent CD-layer capsules filled with pure ^3He. The gaseous fuel was filled to initial densities of (a) 2.5 mg/cm^3 and (b) 0.5 mg/cm^3. The CH capsule histories show distinct times of D^3He nuclear production corresponding to the shock (at ~1.5 ns) and compression (~ 1.75 ns) burns. CD capsule implosions require mixing of the fuel and shell on the atomic scale for D^3He production, and the histories show that no such mix has occurred at shock-bang time. The time necessary for hydro-instabilities to induce fuel-shell mix results in a typical 75±30 ps delay in the peak D^3He reaction rate in CD capsules compared to equivalent CH capsules. In addition, nuclear production in CD implosions continues even after the compression burn ends in CH capsules, staying well above the typical noise level of 3×10^{15}/s for an additional 50 ps.

The higher RT-induced mix susceptibility of capsules filled to lower initial density was observed for a wide range of capsule parameters, as shown in Fig. 13 and as described in Ref. 33. With our colleagues at Los Alamos National Laboratory, the results of these experiments were compared to a multi-fluid interpenetration mix model, where the calculated results also demonstrated increasing mix for

lower initial densities, and the experimental observations from D_2, DT, and ^{3}He filled implosions could be matched using a single value of the free parameter in the model [34].

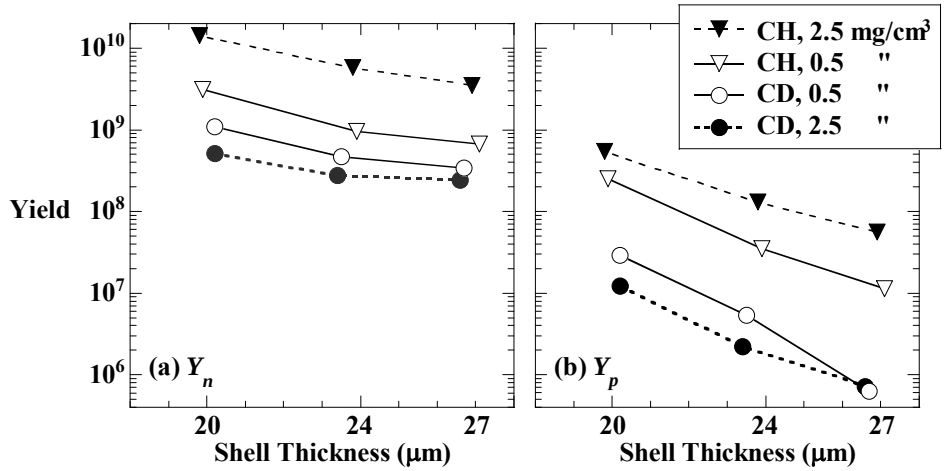

FIG. 13: (a) DD-n and (b) D^{3}He yield in CH (triangles) and CD (circles) capsules with low (open markers) and high (solid markers) ρ_0 as a function of shell thickness. Capsules with lower ρ_0 are more susceptible to mix for all shell thicknesses.

The direct-drive part of SOW Task D is thus complete.

ii. Indirect-drive experiments

Several experimental campaigns involving the use of MIT diagnostics in studying indirect-drive experiments were organized at OMEGA by scientists at Lawrence Livermore National Laboratory, as discussed in Sec. II-A, and Los Alamos National Laboratory. We supported all of their experiments, providing the data they requested, and these campaigns have led to active discussions about future work and this work is ongoing.

E. Other studies of ρR at shock-coalescence time

The goals and objectives of SOW task E have all been reached, as described below and in Secs. II-A and II-B.

Accurate predictions concerning the propagation of convergent shocks are essential for ignition and high gain in ICF. Current ICF ignition designs include a sequence of up to four convergent shocks which must be precisely timed to coalesce at the inner shell surface so as to obtain maximal shell compression, a necessity for high fusion gain. All shocks formed after the first must propagate through already-shocked material, which introduces uncertainty into the shock speed and strength. Thorough understanding of shock speeds in cold and heated material, and in planar and convergent geometries, will be vital for satisfactory ICF implosion performance.

Nuclear production induced by the collapse of strong, spherically convergent shocks was observed using temporal and spectral measurements of products from two distinct nuclear reactions (Fig. 14) [35]. The dual nuclear observations create a comprehensive description of the state of the implosion at shock collapse time, immediately before the onset of the deceleration phase, and revealed numerous differences from predictions made by 1D hydrodynamic simulations. Measurements demonstrated that shock collapse occurs 200-350 ps earlier, that nuclear production is 8 to 30 times lower, and that capsule compression as measured by the areal density ρR is only half of what simulations predict (Fig. 15). Although adjustments to the simulation flux limiter can be made to match the timing, no value of the flux limiter can match the shock timing, yield, and ρR simultaneously. Measuring both DD and D^{3}He nuclear

products allowed a shock temperature near 6 keV to be inferred, and acts as a powerful constraint and verification of data reliability. Given the importance of shock timing and heating to the success of ignition in ICF, it is worthwhile to reexamine the treatment of shocks in current hydrodynamic codes; the constraints imposed by this compelling set of dual nuclear shock burn measurements allows efficient and insightful alterations to be selectively made in ICF simulations at a level hitherto unavailable.

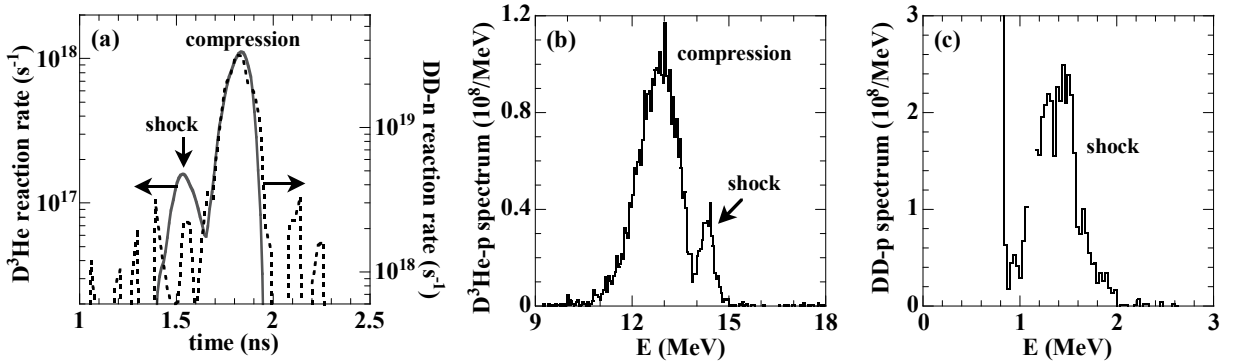

FIG. 14.: Shock ρR values for 18 atm and 3.6 atm D^3He fills of capsules with various shell thickness. The experimental ρR_{sh} is inferred from the downshift of (a) 14.7 MeV D^3He protons and (b) 3 MeV DD-protons from their birth energy. Markers show mean and standard error. (c) The simulated ρR is the ρR of the implosion weighted by the D^3He reaction rate over the shock burn.

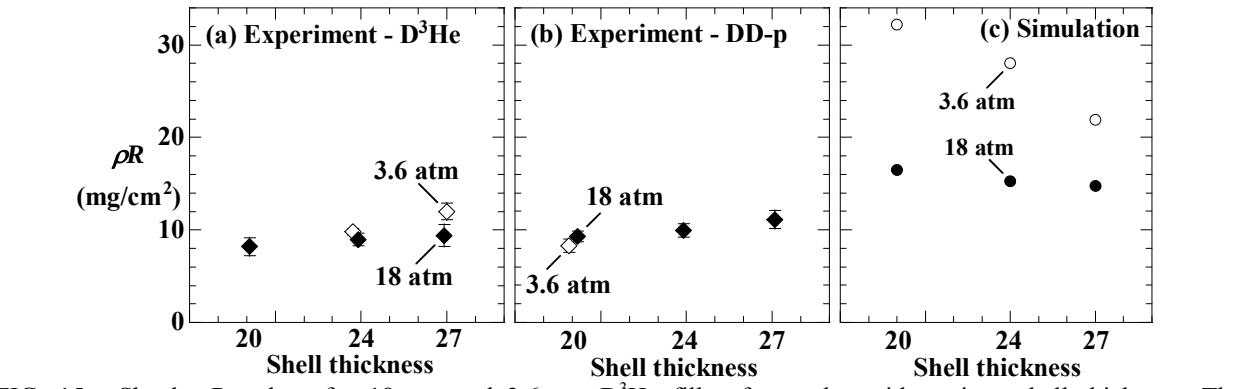

FIG. 15. Shock ρR values for 18 atm and 3.6 atm D^3He fills of capsules with various shell thickness. The experimental ρR_{sh} is inferred from the downshift of (a) 14.7 MeV D^3He protons and (b) 3 MeV DD-protons from their birth energy. Markers show mean and standard error. (c) The simulated ρR is the ρR of the implosion weighted by the D^3He reaction rate over the shock burn.

F. New and upgraded diagnostics

The goals and objectives of SOW task F have all been reached, as described below.

i. Magnetic Recoil Spectrometer (MRS) for high-resolution neutron spectroscopy for ρR and T_i on OMEGA, OMEGA-EP, and the NIF

A Magnetic Recoil Spectrometer (MRS) is being built at OMEGA for measurements of primarily scattered neutrons in the energy range 6-10 MeV, from which areal-density (ρR) can be inferred. The spectrometer covers the energy range from 6 to 32 MeV, enabling simultaneous measurements of scattered, primary and tertiary neutrons. The MRS, which based on a magnet purchased under this DoE grant, is about to be installed on OMEGA for testing, debugging, and verification that all the necessary elements of the MRS are functioning. See Sec. II-I for details.

ii. Proton emission imaging cameras

As indicated in Sec. II-F-ii, both hardware and analysis software have been developed for imaging the burning core of imploded D^3He-filled capsules [21,22,23,25], and this technique has been used to study how laser drive conditions and capsule parameters affect the size and symmetry of the burn region in implosions [22,23,36]. Each camera consists of a round aperture (2000 μm in diameter), about 3 cm from the target, and a sheet of CR-39 as the imaging detector, about 30 cm from the target. The detector is covered with a filter for slowing down protons to the energy range of sensitivity of CR-39. The raw images are penumbral images, which are post processed with MIT-developed algorithms [21,22,23].

The imaging is performed with pinhole cameras in which the recorder consists of stacked sheets of CR-39 nuclear track detector separated by ranging filters that result in efficient detection of 14.7-MeV D^3He protons on one sheet and 3-MeV DD protons on another (see Figs 16a,b). Each camera is interfaced with OMEGA as illustrated in Figure 12c. The image produced directly by a camera is not a direct image of the burn region, because the pinhole is much bigger than the burn region. All information about the burn is contained in the penumbra of the raw camera image, which must be post-processed with special inversion algorithms that reconstruct the distribution of emission in the capsule. We use two approaches. One approach is to assume the emission distribution is spherical, and reconstruct a radial burn profile, as illustrated in Fig. 6. The other approach is to reconstruct two-dimensional images of the surface brightness of the capsule. There are now three cameras that can be mounted in such a way as to image capsules from three orthogonal directions simultaneously for symmetry studies. Data from each are then used to reconstruct a 2-dimensional map of the surface brightness of the capsule, and the three separate images give a good idea of any burn asymmetries (as illustrated in Fig. 7).

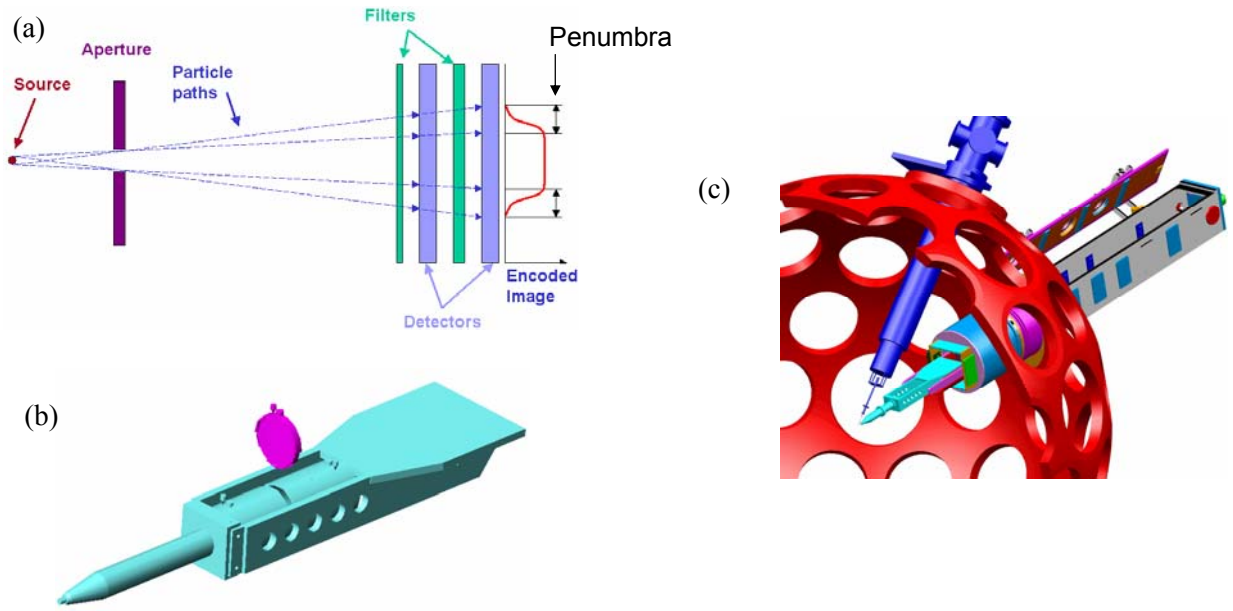

Figure 16: Diagrams illustrating the structure of the proton emission imaging cameras.
(a) Diagram showing the parameters of a penumbral imaging system. Spatial information about an unknown source can be recovered from the penumbra region of the image formed on a detector from an aperture much larger than the size of the source. There are actually two detectors, separated by a filter, so that each detector records information about protons of different energies.
(b) Camera mounting hardware. The pinhole is attached to the front of the assembly, located at the bottom left of the image. The small circular disk, shown removed from the mounting hardware, contains the CR39 nuclear track detectors.
(c) Schematic of the assembled camera hardware in the OMEGA target chamber. The camera mount attaches to the diagnostic port of the OMEGA target chamber. The filter pack and nose cone are attached at the end, and the diagnostic port adjusts to position the entire assembly. On the top is the target positioner, which holds the capsule at the end of a stalk.

iv. New Wedge-Range-Filter (WRF) spectrometers

During the period of the grant, new proton spectrometers have been designed, fabricated, and fielded on OMEGA for study of ρR in cryogenic implosions. Before the current grant, we had developed and perfected the 1st-generation WRF proton spectrometer for high-accuracy (calibration errors < 100 keV), high-resolution measurements of proton spectra in the energy range 8-18 MeV [9,10]. Ten of these, fabricated and calibrated with elaborate procedures (using accelerator-generated protons) [8], are still in constant use after more than five years for primary D^3He protons from D-^{3}He fuel, for secondary D^3He protons from D_2 fuel, and for knock-on protons from 14.1-MeV neutrons from D-T fuel (where the protons come either from the shell or from H added to the fuel). Figure 17a shows the filter part of a WRF assembly.

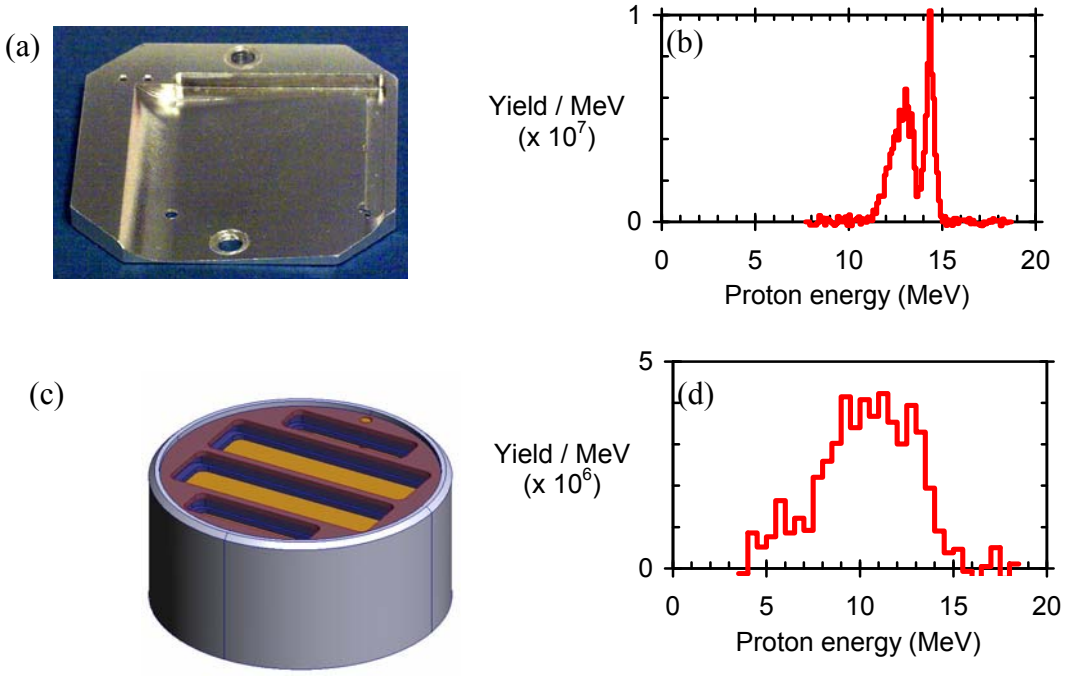

Figure 17. Old and new Wedge-Range-Filter (WRF) proton spectrometers with sample spectra (a) The filter used in the first-generation WRF (the filter is 4 cm wide). The complete spectrometer consists of this filter, a sheet of CR39 detector, and a holding mechanism. The energy range covered is 8-18 MeV. (b) Sample spectrum of D^3He protons acquired with a 1st-generation WRF spectrometer (OMEGA shot 25688, 24-atm of D^3He in a 29-μm CH shell). (c) Drawing of the modular 2nd generation mWRF, designed for the energy range 2 -20 MeV. The four apertures shown on the top surface can accommodate different wedge-shaped filters, and the diameter of the module is 5 cm. (d) Sample spectrum of secondary D^3He protons from a cryogenic D_2 shot at OMEGA acquired with a 2nd-generation mWRF spectrometer (OMEGA shot 47210).

Each first-generation WRF consists of a CR-39 nuclear track detector behind an aluminum filter with a wedge-shaped cross section varying in thickness from 400 μm to 1800 μm. By utilizing the relationships between filter thickness, incoming-proton energy loss in the filter, and the energy-resolving characteristics of CR-39, it is possible to reconstruct the spectrum of incident protons [8]. The simplicity and compactness of each WRF makes possible placement close to a target for use with low proton yields (as low as 10^6) and/or at many positions in the target chamber for symmetry measurements (see Figs 1,2,3,4,5,13,25). Figures 1,2,4,5,13,24 show sample spectra made with these spectrometers.

During the grant, a special version of the first-generation WRF was made in a small format for operation close to target chamber center (~ 5 cm) for studying indirect-drive experiments at OMEGA

[19,20]. The desire to get closer to the target than the standard WRFs allowed (~10 cm) was that the yields are low and getting closer could theoretically give us better statistics. Twelve of these spectrometers were used in experiments, but it was eventually decided that better performance could be obtained by using the standard WRFs at their closest distance of ~ 10 cm (see Fig. 5b). The reason is that they were more easily calibrated and would cover nearly the same solid angle as seen from the target.

The first-generation WRFs have been extraordinarily useful, and their energy ranges have been satisfactory for most experiments until a year or so ago (with capsule areal densities up to ~ 100 mg/cm^2). But cryogenic implosions at OMEGA were predicted several years ago to achieve ρR ~ 200 mg/cm^2, and measurement of their secondary proton spectra requires coverage down to ~ 4 MeV or lower. So new spectrometers, called mWRFs (m for "modular"), were designed to cover the energy range 2-20 MeV. Figure 17c illustrates the structure of the filter-holding module, which allows for different types of filters to be used for different applications. The primary component used in this module is a special Zirconia wedge filter. Twenty four of them have been fabricated and have received preliminary calibrations based on exposures at the MIT accelerator (Sec. II-G) and on OMEGA. They are now used routinely as the primary diagnostic for determining ρR and ρR symmetry of D_2 cryogenic implosions on OMEGA, providing accurate measurements of the secondary proton spectra from multiple directions (Fig. 17d).

vi. New methods for scanning and analyzing CR-39

Most of our charged-particle diagnostics rely on CR-39 nuclear track detectors, which are basically sheets of a clear plastic in which the particles leave trails of damage sites. After etching in NaOH, the location where each particle entered the surface becomes a conical hole which can be identified and quantified in a digitized microscope image. The diameter of the hole, or track, varies with the particle energy, so these detectors allow us to see exactly where each particle entered and what its energy was (within a certain range of energy sensitivity). Before the grant, we used scanning systems based on microscopes fitted with an analog video camera and requiring either manual focus or an interpolation-based focus. The resolution and focus accuracy of this system have limited our ability to consistently identify and quantify the small tracks that are generated by high-energy particles, and also our ability to discriminate small particle tracks from certain kinds of "intrinsic noise" in the form of defects in the CR-39 that look like real tracks. We've now developed a new system utilizing a digital video camera providing a much higher spatial resolution (about 0.2 μm, giving about 10 times as many pixels per unit area) and with a new, very accurate, laser-based autofocus system. Together with completely new software, this system has already provided data of far higher sensitivity and consistency than previously possible. It has been especially helpful for proton imaging camera data.

The new scanning software provides a wider range of data than the old software, and new analysis software has been written to accommodate the scan data and to analyze the data in new ways.

G. Upgrade of the MIT 170-kV Cockcroft-Walton accelerator for developing, testing, and calibrating ICF diagnostics, and for training students

MIT's Fusion Product Source (FPS), shown in Fig. 18, has been used extensively in our program for developing, testing, and calibrating ICF diagnostics [37,38]. In fact, MIT has never fielded an instrument at either NOVA or OMEGA without first validating and calibrating it at the FPS. We have made the following upgrades, which meet the goals and objectives of SOW task G.

- The accelerator tube was replaced.
- A new and highly-flexible target chamber was designed and constructed (see Fig. 18b).
- The drift tube was extended to accommodate new beam diagnostics and a significantly larger and more versatile target chamber.
- A new vacuum and valve system was implemented.
- The target was redesigned for the new chamber and to improve cooling. An automated position control system was also developed for the target.

- A new gas feed system was developed with safety, conservation, and modularity as the focus.
- A Faraday cup was designed and implemented for beam current measurements.
- A gas analyzer was purchased for monitoring contaminates in the chamber.
- The power system was completely redesigned and a new system built.
- Many control and monitoring electronics were implemented with computer control and measurement in mind.
- All control and measurement is now done through software we developed.

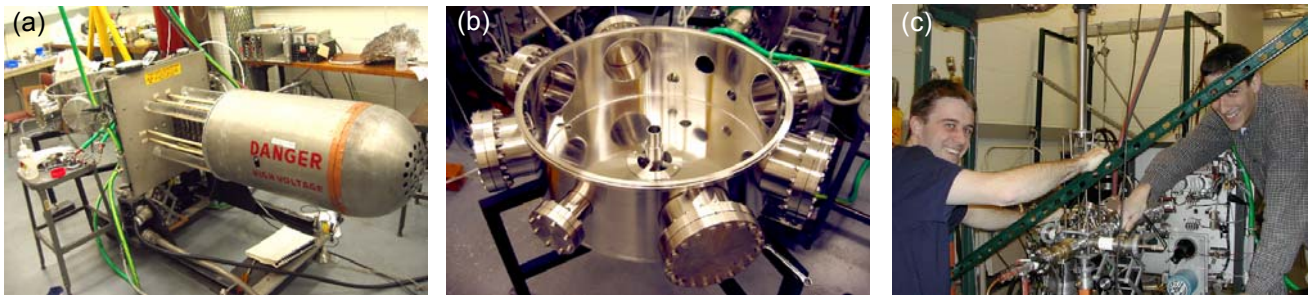

FIG. 18. (a) The MIT Fusion Product Source (FPS) will be used to test, validate, and calibrate all proposed diagnostics. (b) The new target chamber that will be used for CR-39 coincidence tests and WRF spectrometer calibrations. (c) Graduate students Ryan Rygg and Joe DeCiantis, both winners of Excellence Awards for Implosion Research at the last NNSA Symposium, working at the FPS.

H. Graduate and undergraduate student training, education and research

The MIT group has outstanding graduate and undergraduate students training in ICF and HEDP. They are involved in a wide range of projects from experimental to simulation to theory. The graduate students are deeply engaged in every aspect of our research program, and spend considerable time at LLE working on experiments and working with our collaborators from LLE and from the National Labs. They report their results at the major conferences (DPP, Anomalous, IFSA, HTPD), at National Laboratory workshops and seminars, and at seminars at MIT and LLE, and they write up their work for submission to refereed physics journals. Each graduate student typically has three major first-author publications as well as co-authorship on several (typically 5-7) other major publications by the completion of their thesis. During the grant period we had the eight graduate students shown on the chart in Sec. III. Graduate students Ryan Rygg and Joe DeCiantis both were awarded 1st Place Excellence Awards for their Graduate Research at NNSA symposia, and Ryan Rygg finished his degree last year. He has worked with us a postdoc since then, and we expect that next year he will work at one of the national laboratories. His PhD thesis has been nominated for the Marshall Rosenbluth outstanding thesis award.

We have found that the undergraduates are also quite eager to participate and to learn about ICF. The MIT Fusion Product Source gives them hands-on experience with many of the techniques we are using at, or developing for, OMEGA and the NIF. At least 18 undergraduates worked in our group during the grant period (see Sec. III). Each had a project for which he or she had primary responsibility, and one (A. McGlaughlin) is currently writing a senior thesis based on his project.

The goals and objectives of SOW task H have been reached.

I. Purchase of the Magnet for a Magnetic-Recoil Spectrometer

The OMEGA-MRS is a replica and prototype of the MRS system we will to interface at the NIF in 2011 ("NIF-MRS") except for some rescaling of distances. The OMEGA-MRS is currently being interfaced at OMEGA, using the magnet purchased under this grant. The purchase order was issued on 14 July 2004, and the magnet was delivered at OMEGA on 31 January 2005. The goals and objectives of the SOW for the magnet have thus been reached.

i. Development of a NIF prototype neutron spectrometer at OMEGA

Measurement of ρR is fundamental to understanding the performance of any type of implosion [1,2]. MIT and collaborators have developed and utilized charged-particle diagnostics for determining ρR (see Secs. II-F-iv, II-A, II-E, II-J-iv and Ref. 8), but they will fail for ρR > 200 mg/cm^2 and will therefore not work for the ~300 mg/cm^2 expected in upcoming OMEGA cryogenic DT implosions, or the 300-2000 mg/cm^2 expected in NIF implosions. MIT therefore proposed and undertook the design of a unique high-resolution neutron spectrometer for measurements of primarily scattered neutrons, from which ρR in the 100 to 2000 mg/cm^2 range can be inferred [39-42].

After several reviews by National Laboratory participants and the DP office, MIT contracted Dexter Magnetic Technologies, a couple of years ago, to fabricate the most expensive component, which is a magnet. The MRS project at UR/LLE is now a program comprised of a couple concurrent efforts including the engineering of the MRS, and developing a new detection technique with improved signal-to-background characteristics. With the commitment of LLE to engineer the interface of the spectrometer to OMEGA, we anticipate interfacing and qualifying the instrument on OMEGA in July this year.

The instrument is called the Magnetic Recoil Spectrometer (MRS) because of its operating principle, shown in Fig. 19a. The prototype ("OMEGA-MRS") and its planned interface on OMEGA have been designed, as shown in Fig. 1b. CR-39 will be used for particle detection. The nature of the spectra to be measured is illustrated in Fig. 20, which shows simulations from our LLNL collaborators for a cryogenic DT implosion at OMEGA (ρR≈130 mg/cm^2), a NIF fizzle (ρR~1000 mg/cm^2), and an ignited capsule (ρR~1500 mg/cm^2). The MRS should be able to reliably measure all of these spectra for determination of ρR, T_i, and absolute yield as described in Ref. 40.

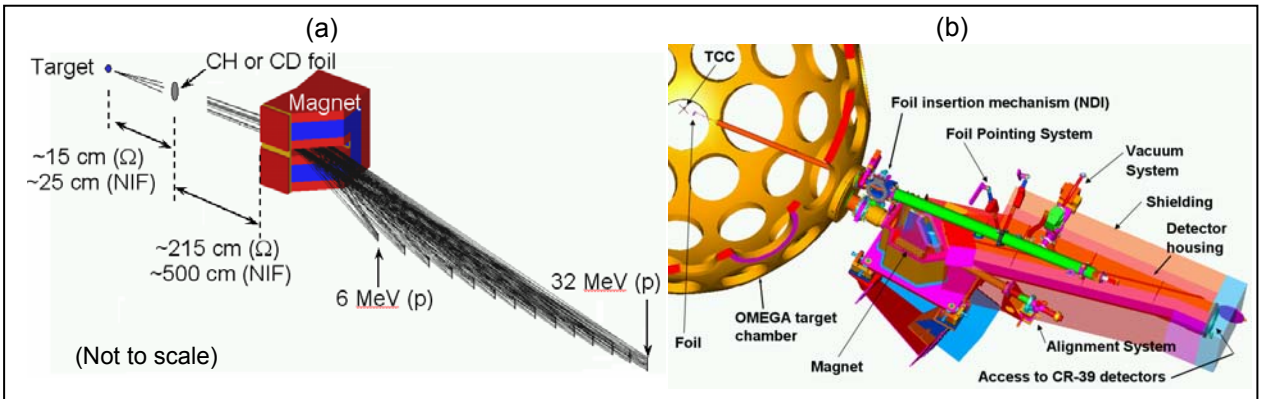

FIG. 19. (a) Principle of the Magnetic Recoil Spectrometer (MRS), which will be used to determine ρR, T_i, and the absolute neutron yield with high accuracy, first at OMEGA, then at the NIF. Forward scattered protons (or deuterons) from a CH foil (or CD foil) are momentum analyzed and focused by the magnet onto the detector. The magnet for the OMEGA system has been fabricated [39-42]. (b) Engineering design for MRS system on OMEGA. With the commitment of LLE to engineer the interface of the spectrometer to OMEGA, we anticipate interfacing and qualifying the instrument on OMEGA in July this year.

The OMEGA-MRS is a replica and prototype of the MRS system we will to interface at the NIF in 2011 ("NIF-MRS") except for some rescaling of distances. The magnet, which is the core of the spectrometer, is virtually identical for both systems. Well before 2010 we must test, debug, and verify at OMEGA that all the necessary elements of the MRS are functioning flawlessly; these include the detector, the full system integration, the analysis programs, the instrument calibration, and the final instrument qualification. Very important to this process is cross calibration between MRS and charged particle measurements for cryogenic DT implosions with ρR~100 to 200 mg/cm^2, where both approaches will work. When cryogenic DT operates above 200 mg/cm^2, only the MRS will be able to measure the ρR; its utility will be unique and vital to implosion studies and the National ICF Program.

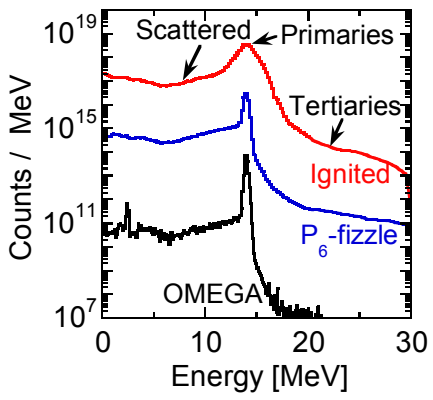

FIG. 20. Simulated neutron spectra that could be measured by the neutron spectrometer (MRS). The three spectra are for an ignited implosion with ρR ~1500 mg/cm^2 (S. Haan), a NIF "P_6-fizzle" with ρR~1000 mg/cm^2 (S. Haan), and an OMEGA cryogenic DT implosion with ρR≈130 mg/cm^2 (S. Hatchett). In each case, the MRS will accurately measure ρR, T_i, and absolute yield [40]. As the MRS energy range is 6-32 MeV, independent determinations of NIF ρR can be made through both scattered and tertiary neutrons. For the P_6 fizzle, the scattered neutron spectra differ in different directions, reflecting the ρR asymmetries. Orthogonal-viewing MRS systems would be sensitive to these distortions [40].

ii. Principles of operation and scientific objectives

The MRS has three basic components, as indicated in Fig. 19a [40]. The first is a CH (or CD) foil to produce recoil protons (or deuterons) from incident neutrons. The second is a magnet for energy dispersion and for focusing of forward-scattered recoil particles onto a detector plane. This focusing provides a clear mapping between position in the plane and the energy of the proton (or deuteron), and thus the energy of the neutron that scattered it. The third is the detector, which must record the position of each recoil particle and be insensitive to various sources of background; for this we will use CR-39 nuclear track detectors in coincidence mode. Important to the design is the fact that the MRS measures spectra of neutrons between 6 and 32 MeV, covering all essential details of the three simulations shown in Fig. 20. For example, from NIF tertiaries [5] a second estimate can be independently made of the fuel ρR. This can be directly compared to the principal method of ρR determination from the scattered primaries. Having such self-consistency checks could prove immensely important for NIF fizzles. In addition, the absolute primary yield and a highly resolved 14.1 MeV primary neutron spectrum can be measured at both OMEGA and the NIF, making possible precise estimates of the ion temperature and (possibly more interestingly) any deviations from a single temperature.

J. Accomplishments not anticipated in the original Statement of Work

The work performed under this grant often led us in new directions, resulting in a large number of projects and accomplishments in the areas of diagnostic development and physics research that were not anticipated when the proposals were written. A few of them are described below (and in the publications and conference presentations listed in Secs. IV and V).

i. Proton Temporal Diagnostic (PTD)

To advance our understanding of implosion dynamics and to impose exacting tests on simulations, it is important to have measurements of shock and compression bang time, of shock and compression yield, and of the time dependence of ρR and T_i. With this goal in mind, our group and collaborators have recently developed the Proton Temporal Diagnostic (PTD) and analysis techniques [14]. The operational principle of the PTD is shown in Fig. 21.

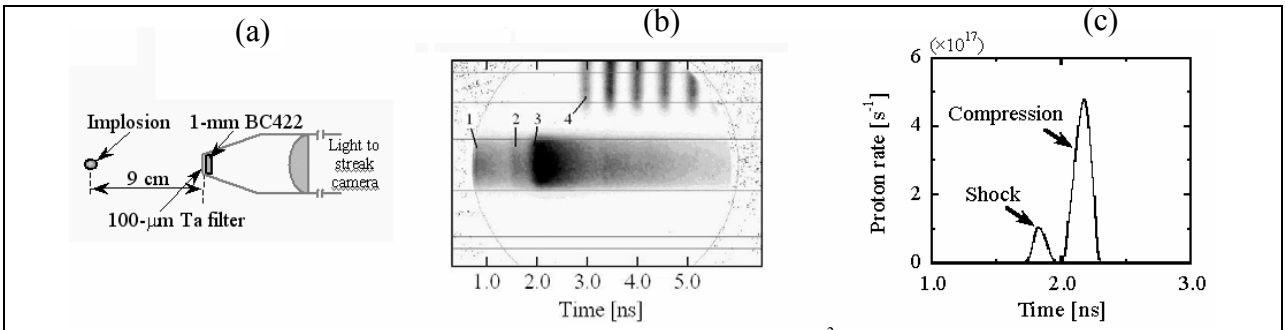

FIG. 21. The proton temporal diagnostic (PTD) for measurements of the D^3He burn history. (a) The PTD front end. (b) Streaked image of scintillator output, recorded by a CCD camera attached to a streak camera. (c) Resulting time history of the D^3He burn, indicating both shock burn and compression burn for shot 31271. In (b), a train of optical fiducial signals (labeled "4"), is used for timing reference. Also indicated is the x-ray component (labeled 1), shock component (labeled 2), and compression component (labeled 3).

Because the T_i dependence of the D^3He reaction is much stronger than that of the DD reaction, shock bang time can be measured far more accurately from the proton rate in D^3He implosions than from the neutron rate from either DD or DT implosions. Shock bang is particularly important because it is unaffected by mix [15] and is also one of the best measures of drive efficiency. As an illustration, Fig. 22 shows an example of a PTD-measured proton rate history from a D^3He implosion, and 1-D LILAC simulations of the same implosion. Selection of an appropriate flux limiter (in this case 0.07) results in a simulation that matches the timing of shock bang and compression bang, but the yield does not agree even for the shock bang (at which time the 1-D calculation would be expected to be at its most accurate because of the absence of mix).

In the future we will carry out similar measurements for a variety of D^3He implosions and compare them to both 1-D and multi-dimensional simulations to see if any simulations can match all the parameters of the data including timing, burn durations, and yields. In addition, for optimized ratios of D and ^3He (i.e. a predominance of D), the DD burn history can be measured (by the neutron temporal diagnostic [43]) in addition to the D^3He burn history for more constraints on the simulations. Although the DD shock yield is low and may be hard to measure accurately, we will utilize both the DD and D^3He burn rates in comparisons to both 1-D and multi-dimensional simulations.

FIG. 22. The first measured D^3He burn rate histories provide clear shock bang timing and a new and stringent test of simulations. In this case, the measurement (solid red) is compared with two 1-D simulations with flux limiters of 0.06 and 0.07 (dashed lines) for a 24-μm thick CH shell implosion (shot 29839). The shock and the compression bang times are well matched by the 1-D calculation with flux limiter 0.07, but neither simulation (nor others not shown) can match the magnitude of the shock burn, for which there is no mix and 1-D should be expected to best replicate the experiment.

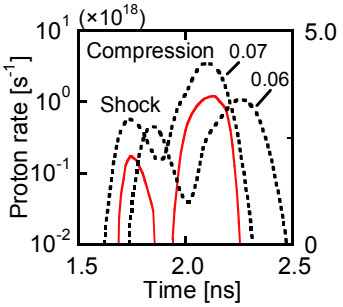

ii. Compact neutron spectrometers

To take advantage of the EMP insensitivity of CR-39 for use in neutron spectroscopy, which is very important for OMEGA-EP, Z, NIF, and even many OMEGA experiments, we tested a prototype "neutron WRF spectrometer" (nWRF). It is based on the idea that a proton recoil foil, made of CH, is placed in front of a WRF. Thus forward-scattered recoil protons are energy analyzed by the WRF. Extremely important is the fact that the nWRF is very compact; the distance between the CH foil and WRF is ~ 30 cm; this allows great flexibility in its deployment.

Proof-of-principle experiments at OMEGA for DT shots are shown in Fig. 23. Though the design was unoptimized, there is very acceptable agreement between T_i determined from the nWRF and the standard time-of-flight diagnostic. In future work, we will optimize the design, and build a small set, of nWRFs appropriate for Z, OMEGA-EP, OMEGA, and eventually for the NIF, with the goal of providing high-resolution measurements of primary and secondary neutrons.

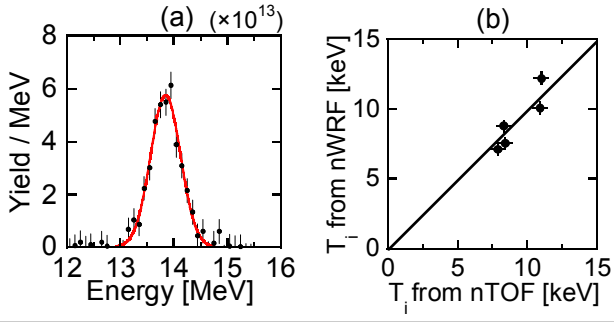

FIG. 23. (a) First proof-of-principle measurements of a DT neutron spectrum, obtained from a compact, EMP-resistant spectrometer (see text). The technique involves measuring forward scattered recoil protons with a WRF spectrometer. (b) Comparison of T_i determined from nWRF and neutron time-of-flight. (Due to energy loss in the recoil CH foil, the spectrum in (a) is downshifted by about 200 keV.)

iii. Measurements of ion temperature evolution

An immediate application of the PTD is to determine the evolution of the ion temperature $T_i(t)$ from the ratio of absolute DD and D^3He burn rates, making small corrections for volumetric effects of the different DD and D^3He burn regions [14,44]. Figure 24 illustrates such data and a comparison to 1-D LILAC implosion simulations for 20 μm and 27 μm thick CH shells. It is interesting that the match to 1-D is much better for the 27-μm case; this may reflect the reduced effects of mix for thicker, more stable implosions [3,4,24,45]. In the future we will perform systematic studies of such $T_i(t)$ evolution for a variety of implosions, and to compare in detail to 1-D and multi-dimensional simulations. Attempts will also be made to extend time-evolving temperature determinations into the shock burn region.

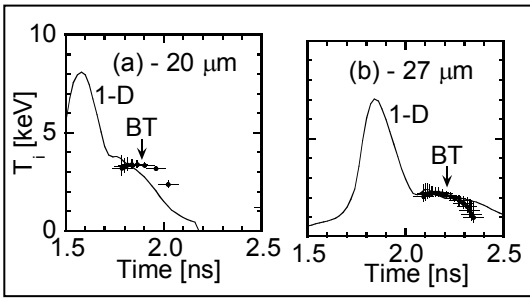

FIG. 24. The first measurements of ion temperature evolution are providing new insights into the effects of capsule stability on mix. $T_i(t)$ is determined from the ratio of measured DD and D^3He burn histories for implosions of capsules with (a) 20-μm and (b) 27-μm-thick shells. For the 27-μm case, the match with 1-D at compression bang time (BT) is quite good, probably reflecting the reduced effects of mix [14].

iv. Measurements of mass assembly in cone-in-shell implosions for Fast Ignition

The reentrant cone-in-shell concept [46-48] is a novel approach to fast ignition (FI) [49], separating fuel-assembly from fuel heating by combining a driver that compresses the fuel to high density with an ultra-fast laser for heating. Charged-particle diagnostics have begun to play a unique role in assessing the mass assembly by measuring ρR and ρR asymmetries, as demonstrated by recent experiments at OMEGA [50]. Figure 25 shows, at time of peak proton production, an image of an imploded 10-atm D^3He-filled cone target made with a 6.7-keV x-ray backlighter. The measured energy loss of 14.7-MeV D^3He protons was used to infer the ρR of the compressed capsule [44] in different directions. The narrow peak seen at the high-energy end of the spectra is attributed to the shock phase of the implosions, at which time the assembled ρR is low. At lower energies, there is a second broad peak

attributed to the compression phase of the implosion. Of the five views of this implosion, TIM3 shows the largest compression downshift (~2 MeV), corresponding to ρR = 60±10 mg/cm^2. These measurements quantitatively demonstrate the anisotropy in the mass assembly.

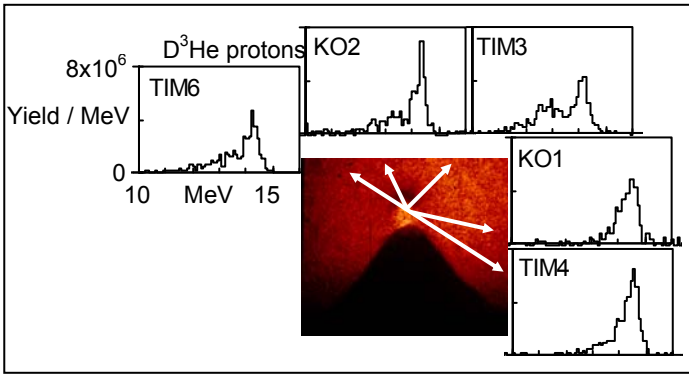

FIG. 25. D^{3}He proton spectra obtained along 5 different lines of sight for a 10-atm D^{3}He-filled cone-in-shell implosion indicate ρR asymmetries, with the largest compression ρR in the direction of TIM3 (60±10 mg/cm^2). The x-ray image is a result of a 6.7-keV x-ray backlighter and plasma self emission.

v. Theoretical studies of energy deposition of energetic electrons in hydrogenic plasmas

For fast ignition to work, ~1-MeV electrons must efficiently deposit their energy in a high-density (~ 300 g/cm^3) DT plasma that has been pre-compressed. With this issue in mind, we recently published analytic calculations that predict electron stopping power and penetration [51]. In addition, we calculated the longitudinal straggling and the blooming of mono-energetic (0.3 to 5 MeV) electron beams interacting with a homogeneous, dense DT plasma [52]. Figure 26 illustrates the stopping power and penetration (400 mg/cm^2 or 14 μm) for 1-MeV electrons. The two results shown are from the continuous-slowing down model (thin line), which is very close to the original formulation used by Tabak *et al.* [49], and our new model heavy line) that includes the effects of scattering off both electrons and ions. For Z=1 fast-ignition plasmas, scattering off background electrons is just as important as off ions. In the future we will attempt to quantitatively apply this model to simulations of FI assembled mass, such as recently presented [53], in order to establish rigorous ignition requirements.

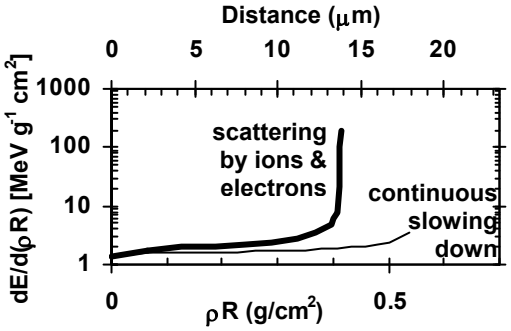

FIG. 26. New MIT calculations of electron stopping power have important implications for establishing fast-ignition requirements. Shown here is the stopping power for 1-MeV electrons, plotted as a function of the electron penetration, for a DT plasma with ρ=300 g/cm^3 and T_e=5 keV [51]. The new results (heavy line) predict a penetration of 400 mg/cm^2 (or 14 μm), which is 35% smaller than the standard calculated value (thin line).

III. TEAM MEMBERS

MIT Scientists	Technical Staff	Graduate Students	Undergraduate Students
Dr. Richard Petrasso	Michael Canavan	Cliff Chen	Greg Belote
Dr. Chikang Li	Jocelyn Schaeffer	Larissa Cottrill	Molly Bright
Dr. Fredrick Seguin	Randy Leiter	Joseph DeCiantis	Dylan Consla
Dr. Johan Frenje	Sean McDuffee	Shinya Kurebayashi	Daniel Denis
	Irina Cashen	J. Ryan Rygg*	Magnus Falk
		Daniel Casey	Jessica Lam
		Mario Manuel	Andy McLaughlin
		Brook Schwartz	Rory Rother
			Amy Slagle
			Siddarth Sundar
			Gabriel Warshauer-Baker
			Jon Williams
			Jeffrey Perez
			Sohrab Virk
			Jeremy Chang
			Jeremy Jacox

* Received his PhD in October 2006, and since then has been a postdoc in our group.

IV. GROUP PUBLICATIONS DURING THE PERIOD OF THE GRANT

Note that many of our papers are available on our Internet site at the URL "http://psfcwww2.psfc.mit.edu/physics_research/hedp/Papers/Papers.html".

In preparation for submission:

1. J.A. Frenje *et al.*, "A magnetic recoil spectrometer (MRS) for absolute measurements of the neutron spectrum from which ρR, Ti and yield can be inferred for cryogenic DT implosions at OMEGA and the NIF".
2. F. H. Séguin *et al.*, "Proton radiography options for OMEGA EP".
3. J.A. Frenje *et al.*, "Diagnosing ρR and ρR modulations of the ablator for failed NIF implosions using charged-particle spectrometry".
4. F. H. Séguin *et al.*, "Angular distributions of areal density in ICF implosions with asymmetric drive".
5. J. R. Rygg *et al.*, "Monoenergetic proton radiography of cone-in-shell implosions".
6. R.D. Petrasso *et al.*, "Monoenergetic proton radiography of direct-drive capsule implosions".
7. F. H. Séguin *et al.*, "Electromagnetic fields outside imploded ICF capsules".
8. C. K. Li and R.D. Petrasso, "Effects of Fast Electron Energy Loss on Interactions in Plasmas".
9. F. H. Seguin *et al.*, "Target shimming for control of ICF implosion symmetry".
10. J.R. Rygg *et al.*, "Observations of the collapse of asymmetrically-driven convergent shocks".
11. J.A. Frenje *et al.*, "Diagnosing cryogenic DT implosions at OMEGA using charged-particle spectrometry".
12. D.T. Casey *et al.*, "Background characterization and reduction for the Magnetic Recoil Spectrometer (MRS) at OMEGA and the NIF".

Submitted:

13. J.R. Rygg, J.A. Frenje, C. K. Li, F. H. Séguin, R. D. Petrasso, J. A. Delettrez, D. D. Meyerhofer, T.C. Sangster, and C. Stoeckl, "Dual nuclear product observations of shock collapse in inertial confinement fusion", submitted to ***Phys. Rev. Lett.*** (2007).
14. C. K. Li, F. H. Séguin, R. P. J. Town, R. D. Petrasso, J. A. Frenje, J. P. Knauer, O. L. Landen, J. R. Rygg, V. A. Smalyuk, "Observation of Megagauss Field Topology Changes due to Magnetic Reconnection in Laser-Produced Plasmas", submitted to ***Phys. Rev. Lett*** (2007).

Accepted:

15. C. K. Li, F. H. Séguin, J. A. Frenje, J. R. Rygg, R. D. Petrasso, R. P. J. Town, P. A. Amendt, S. P. Hatchett, O. L. Landen, A. J. Mackinnon, P. K. Patel, M. Tabak, J. P. Knauer, T. C. Sangster, and V. A. Smalyuk, "Observation of the Decay Dynamics and Instabilities of Megagauss Magnetic Field Structures in Laser-Produced Plasmas", accepted for publication in ***Phys. Rev. Lett***. (2007).
16. J. R. Rygg, J. A. Frenje, C. K. Li, F. H. Seguin, R. D. Petrasso, V. Yu Glebov, D. D. Meyerhofer, T. C. Sangster, and C. Stoeckl, "Time-dependent measurements of mix in inertial confinement fusion", accepted for publication in ***Phys. Rev. Lett.*** (2007).
17. C. Chen, C. K. Li, and R.D. Petrasso, "Comparison of solid and plasma linear energy deposition for electron preheat and fast ignition scenarios", accepted in ***J. Applied Physics*** (2007).

Published:

18. J. R. Rygg, J. A. Frenje, C. K. Li, F. H. Seguin, R. D. Petrasso, J. A. Delettrez, V. Yu. Glebov, V. N. Goncharov, D. D. Meyerhofer, P. B. Radha, S. P. Regan, and T. C. Sangster, "Nuclear measurements of fuel-shell mix in inertial confinement fusion implosions at OMEGA", ***Phys. Plasmas*** 14, 056306 (2007).
19. C. D. Zhou, W. Theobald, R. Betti, P.B. Radha, V.A. Smalyuk, D. Shvarts, V. Yu. Glebov, C. Stoeckl, K.S. Anderson, D.D. Meyerhofer, T.C. Sangster, C.K. Li, R.D. Petrasso, J.A. Frenje, and F.H. Seguin, "High-ρR Implosions for Fast-Ignition Fuel Assembly", ***Phys. Rev. Lett.*** 98, 025004 (2007).

20. V.A. Smalyuk, R. Betti, J.A. Delettrez, V. Yu. Glebov, V. N. Goncharov, D.Y. Li, D.D. Meyerhofer, S.P. Regan, S. Roberts, T.C. Sangster, C. Stoeckl, W. Seka, J.A. Frenje, C.K. Li, and R.D. Petrasso, "Experimental studies of direct-drive, low-intensity, low-adiabat spherical implosions on OMEGA", ***Phys. Plasmas*** 14, 056306 (2007).
21. T.C. Sangster, R. Betti, R.S. Craxton, J.A. Delettrez, D.H. Edgell, L.M. Elasky, V.Yu. Glebov, V.N. Goncharov, D.R. Harding, D. Jacobs-Perkins, R. Janezic, R.L. Keck, J.P. Knauer, S.J. Loucks, L.D. Lund, F.J. Marshall, R.L.McCrory, P.W. McKenty, D.D. Meyerhofer, P.B. Radha, S.P. Regan, W. Seka, W.T. Shmayda, S. Skupsky, V.A. Smalyuk, J.M. Soures, C. Stoeckl, B Yaakobi, J.D. Moody, J.A. Atherton, B.D. MacGowan, J.D. Kilkenny, T.P. Bernat, J.A. Frenje, C.K. Li, R.D. Petrasso, F.H. Seguin and D.S. Montgomery, "Cryogenic DT and D2 Targets for inertial confinement fusion," ***Phys. Plasmas*** 14, 058101 (2007.)
22. G. Kyrala, D.C. Wilson, J.F. Benage, M. Gunderson, K. Klare, W. Garbett, S. James, V. Glebov, B. Yaakobi, J. A. Frenje, and R. Petrasso, "Effect of higher z dopants on implosion dynamics: X-ray spectroscopy," ***High Energy Density Physics***(2007), doi:10.1016/j.hedp.2007.02.018.
23. C. K. Li, F.H. Seguin, J.A. Frenje, J. R. Rygg, R.D. Petrasso, R.P.J. Town, P.A. Amendt, S.P. Hatchett, O.L. Landen, A.J. Mackinnon, and P.K. Patel, "Measuring E and B fields in Laser-Produced Plasmas with Monoenergetic Proton Radiography", ***Phys. Rev. Lett.*** 97 135003 (2006).
24. F. H. Seguin, J. L. DeCiantis, J. A. Frenje, C. K. Li, J. R. Rygg, C. D. Chen, R. D. Petrasso, J. A. Delettrez, S. P. Regan, V. A. Smalyuk, V. Yu. Glebov, J. P. Knauer, F. J. Marshall, D. D. Meyerhofer, S. Roberts, T. C. Sangster, C. Stoeckl, K. Mikaelian, H. S. Park, H. F. Robey, and R. E. Tipton, "Measured dependence of nuclear burn region size on implosion parameters in inertial confinement fusion experiments", ***Phys. Plasmas*** 13 , 082704 (2006).
25. C. K. Li and R. D. Petrasso, "Energy deposition of MeV electrons in compressed targets of fast-ignition inertial confinement fusion", ***Phys. Plasmas*** 13 , 056314 (2006).
26. J. R. Rygg, J. A. Frenje, C. K. Li, F. H. Séguin, R. D. Petrasso, J. A. Delettrez, V. Yu Glebov, V. N. Goncharov, D. D. Meyerhofer, S. P. Regan, T. C. Sangster, and C. Stoeckl, "Tests of the hydrodynamic equivalence of direct-drive implosions with different D_2 and ^3He mixtures", ***Phys. Plasmas*** 13 , 052702 (2006).
27. V. Yu. Glebov, D. D. Meyerhofer, T. C. Sangster, C. Stoeckl, S. Roberts, C. A. Barrera, J. R. Celeste, C. J. Cerjan, L. S. Dauffy, D. C. Eder, R. L. Griffith, S. W. Haan, B. A. Hammel, S. P. Hatchett, N. Izumi, J. R. Kimbrough, J. A. Koch, O. L. Landen, R. A. Lerche, B. J. MacGowan, M. J. Moran, E. W. Ng, T. W. Phillips, P. M. Song, R. Tommasini, B. K. Young, S. E. Caldwell, G. P. Grim, S. C. Evans, J. M. Mack, T. J. Sedillo, M. D. Wilke, D. C. Wilson, C. S. Young, J. L. Bourgade, L. Disdier, M. Houry, I. Lantuejoul, O. Landoas, G. A. Chandler, G. W. Cooper, R. J. Leeper, R. E. Olson, C. L. Ruiz, M. A. Sweeney, S. P. Padalino, C. Horsfield, B. A. Davis, D. Casey, J. A. Frenje, C. K. Li, R. D. Petrasso, and F. H. Séguin, "Development of nuclear diagnostics for the National Ignition Facility (invited)", ***Rev. Sci. Instrum.*** 77, 10E715 (2006).
28. R. Betti, K. Anderson, T.R. Boehly, T.J.B. Collins, R.S. Craxton, J.A. Delettrez, D.H. Edgell, R.Epstein, V. Yu Glebov, V.N. Goncharov, D.R. Harding, R.L. Keck, J.H. Kelly, J.P. Knauer, S.J. Loucks, J.A. Marozas, F.J. Marshall, A.V. Maximov, D.N. Maywar, R.L. McCrory, P.W. McKenty, D.D. Meyerhofer, J. Myatt, P.B. Radha, S.P. Regan, C. Ren, T.C. Sangster, W. Seka, S. Skupsky, A.A. Solodov, V.A. Smalyuk, J.M. Soures, C. Stoeck, W. Theobald, B Yaakobi, C. Zhou, J.D. Zuegal, J. Frenje, C.K. Li, R.D. Petrasso, and F.H. Seguin "Progress in hydrodynamics theory and experiments for direct-drive and fast ignition inertial confinement fusion," ***Plasma Phys. Control Fusion*** 48, B153 (2006).
29. C. K. Li and R. D. Petrasso, "Stopping, straggling, and blooming of directed energetic electrons in hydrogenic and arbitrary-Z plasmas", ***Phys. Rev. E*** 73, 016402 (2006).
30. C. K. Li, F. H. Séguin, J. A. Frenje, J. R. Rygg, R. D. Petrasso, R. P. J. Town, P. A. Amendt, S. P. Hatchett, O. L. Landen, A. J. Mackinnon, P. K. Patel, V. A. Smalyuk, J. P. Knauer, T. C. Sangster, and C. Stoeckl, "Monoenergetic proton backlighter for measuring E and B fields and radiographing implosions and high-energy density plasmas (invited)", ***Rev. Sci. Instrum.*** 77, 10E725 (2006).

31. D. C. Wilson, R. L. Singleton, Jr., J. P. Grondalski, N. M. Hoffman, A. Nobile, Jr., F. H. Séguin, J. A. Frenje, C. K. Li, and R. D. Petrasso, "Diagnosing ablator burn through in ignition capsules using D_2+^{3}He gas filled surrogates", ***Rev. Sci. Instrum.*** 77, 10E711 (2006).
32. V. Tang, J. Liptac, R. R. Parker, P. T. Bonoli, C. L. Fiore, R. S. Granetz, J. H. Irby, Y. Lin, S. J. Wukitch, and The Alcator C-Mod Team, J. A. Frenje, R. Leiter, S.C. McDuffee, R. D. Petrasso, "Compact multichannel neutral particle analyzer for measurement of energetic charge-exchanged neutrals in Alcator C-Mod", ***Rev. Sci. Instrum.*** 77, 083501 (2006).
33. J. L. DeCiantis, J. A. Delettrez, . P. Regan, V. A. Smalyuk, V. Yu. Glebov, J. P. Knauer, F. J. Marshall, D. D. Meyerhofer, S. Roberts, T. C. Sangster, C. Stoeckl, K. Mikaelian, H. S. Park, H. F. Robey, F. H. Séguin, J. A. Frenje, C. K. Li, J. R. Rygg, and R. D. Petrasso, "Proton core imaging of the nuclear burn in inertial confinement fusion implosions", ***Rev. Sci. Instrum***. 77, 043503 (2006).
34. S. Kurebayashi, V. Yu. Glebov, J. A. Delettrez, T. C. Sangster, D. D. Meyerhofer, C. Stoeckl, J. M. Soures, P. A. Amendt, S. P. Hatchett, R. E. Turner, J. A. Frenje, F. H. Seguin, J. R. Rygg, C. K. Li, and R. D. Petrasso, "Using nuclear data and Monte-Carlo techniques to study areal density and mix in D_2 implosions", ***Phys. Plasmas*** 12, 032703 (2005).
35. R.L. McCrory, S.P. Regan, S.J. Loucks, D.D. Meyerhofer, S. Skupsky, R. Betti, T.R. Boehly, R.S. Craxton, T.J.B. Collins, J.A. Delettrez, D. Edgell, R. Epstein, K.A. Fletcher, C. Freeman, J.A. Frenje, V.Yu. Glebov, V.N. Goncharov, D.R. Harding, I.V. Igumenshchev, R.L. Keck, J.D. Kilkenny, J.P. Knauer, C.K. Li, J. Marciante, J.A. Marozas, F.J. Marshall, A.V. Maximov, P.W. McKenty, J. Myatt, S. Padalino, R.D. Petrasso, P.B. Radha, T.C. Sangster, F.H. Séguin, W. Seka, V.A. Smalyuk, J.M. Soures, C. Stoeckl, B. Yaakobi and J.D. Zuegel, "Direct-drive inertial confinement fusion research at the Laboratory for Laser Energetics: charting the path to thermonuclear ignition", ***Plasma Phys. Control. Fusion*** 45, (2005) S283.
36. C. Stoeckl, R. Stephens, J. Delettrez, S. Hatchett, V. Smalyuk, W. Theobald, B. Yaakobi, C. Sangster, C. K. Li, R. D. Petrasso, and F. H. Seguin, "Direct-drive fuel-assembly experiments with gas-filled, cone-in-shell, fast-ignitor targets on the OMEGA Laser", ***Plasma Phys. Control. Fusion*** 47, (2005) B859.
37. V. A. Smalyuk, J. A. Delettrez, S. B. Dumanis, R. Epstein, V. Yu. Glebov, D. D. Meyerhofer, P. B. Radha, T. C. Sangster, C. Stockel, N. C. Toscano, J. A. Frenje, C. K. Li, R. D. Petrasso, and F. H. Seguin, "Hot-core characterization of a cryogenic D_2 target at peak neutron production in a direct-drive spherical implosion", ***Phys. Plasmas*** 12, 052706 (2005).
38. R. B. Stephens, S. P. Hatchett, M. Tabak, C. Stoeckl, H. Shiraga, S. Fujioka, M. Bonino, A. Nikroo, R. Petrasso, T. C. Sangster, J. Smith, and K. A. Tanaka "Implosion hydrodynamics of fast ignition targets", ***Phys. Plasmas*** 12, 056312 (2005).
39. J. P. Knauer, K. Anderson, R. Betti, T. J. B. Collins, V. N. Goncharov, P. W. McKenty, D. D. Meyerhofer, P. B. Radha, S. P. Regan, T. C. Sangster, and V. A. Smalyuk, J. A. Frenje, C. K. Li, R. D. Petrasso, and F. H. Séguin, "Improved target stability using picket pulses to increase and shape the ablator adiabat", ***Phys. Plasmas*** 12, 056306 (2005).
40. F. J. Marshall, R. S. Craxton, J. A. Delettrez, D. H. Edgell, L. M. Elasky, R. Epstein, V. Yu. Glebov, V. N. Goncharov, D. R. Harding, R. Janezic, R. L. Keck, J. D. Kilkenny, J. P. Knauer, S. J. Loucks, L. D. Lund, R. L. McCrory, P. W. McKenty, D. D. Meyerhofer, P. B. Radha, S. P. Regan, T. C. Sangster, W. Seka, V. A. Smalyuk, J. M. Soures, C. Stoeckl, and S. Skupsky, J. A. Frenje, C. K. Li, R. D. Petrasso, and F. H. Séguin, "Direct-drive, cryogenic target implosions on OMEGA", ***Phys. Plasmas*** 12, 056302 (2005).
41. F. H. Séguin, J. L. DeCiantis, J. A. Frenje, S. Kurebayashi, C. K. Li, J. R. Rygg, C. Chen, V. Berube, B. E. Schwartz, R. D. Petrasso, V. A. Smalyuk, F. J. Marshall, J. P. Knauer, J. A. Delettrez, P. W. McKenty, D. D. Meyerhofer, S. Roberts, T. C. Sangster, K. Mikaelian and H. S. Park, "D^3He-proton emission imaging for inertial-confinement-fusion experiments (invited)", ***Rev. Sci. Instrum.*** 75, 3520 (2004).
42. C.K. Li and R.D. Petrasso, "Stopping of Directed Electrons in High-Temperature Hydogenic Plasmas", ***Phys. Rev. E*** 70, 067401 (2004).

43. C. K. Li, F. H. Séguin, J. A. Frenje, R. D. Petrasso, J. A. Delettrez, P. W. McKenty, T. C. Sangster, R. L. Keck, J. M. Soures, F. J. Marshall, D.D. Meyerhofer, N. Goncharov, J. P. Knauer, P. B. Radha, S. P. Regan, W. Seka, "Effects of Nonuniform Illumination on Implosion Asymmetry in Direct-Drive Inertial Confinement Fusion", ***Phys. Rev. Lett.*** 92, 205001 (2004).
44. J. A. Frenje, C. K. Li, F. H. Séguin, J. Deciantis, J. R. Rygg, B.E. Schwartz, S. Kurebayashi, R. D. Petrasso, J. Delettrez, V.Yu. Glebov, F. J. Marshall, D. D. Meyerhofer, T. C. Sangster, C. Stoeckl, J. M. Soures, "Measuring shock bang timing and ρR evolution of D^3He implosions at OMEGA", ***Phys. Plasmas*** 11, 2798 (2004).
45. S. P. Regan, J. A. Delettrez, V. N. Goncharov, F. J. Marshall, J. M. Soures, V. A. Smalyuk, P. B. Radha, B. Yaakobi, R. Epstein, V.Yu. Glebov,P. A. Jaanimagi, D. D. Meyerhofer, T. C. Sangster, W. Seka, S. Skupsky, C. Stoeckl, D. A. Haynes, J. A. Frenje, C. K. Li, R. D. Petrasso, F. H. Seguin, "Dependence of shell Mix on Feedthrough in Direct Drive Inertial Confinement Fusion", ***Phys. Rev. Lett.*** 92, 185002 (2004).
46. P. W. McKenty, T.C. Sangster, M. Alexander, R. S. Craxton, J. A. Delettrez, L. Elasky, R. Epstein, A. Frank, V. Yu. Glebov, D. R. Harding, S. Jin, J. P. Knauer, R. L. Keck, S. Loucks, L. D. Lund, R. L. McCrory, J. Marshall, D. D. Meyerhofer, S. Morse, S. Regan, P. B. Radha, S. Roberts, W. Seka, S. Skupsky, V. A. Smalyuk, J. Soures, M. D. Wittman, J. A. Frenje, C. K. Li, F. H. Seguin, R. D. Petrasso, N. Izumi, J. A. Koch, R. A. Lerche, M. J. Moran, T. W. Phillips, G. J. Schmid "Direct-drive cryogenic target implosion performance on OMEGA", ***Phys. Plasmas*** 11, 2790 (2004).
47. D. Wilson, C. W. Cranfill, C. Christensen, R. A. Forster, R. R. Peterson, N. M. Hoffman, G. D. Pollak, C. K. Li, F. H. Seguin, J. A. Frenje, R. D. Petrasso, P. W. McKenty, F. J. Marshall, V. Yu. Glebov, C. Stoeckl, "Multi-fluid interpenetration mixing in directly driven ICF capsule implosions", ***Phys. Plasmas*** 11, 2723 (2004).
48. C. K. Li, F. H. Seguin, J. A. Frenje, R. D. Petrasso, R. Rygg, S. Kurebayashi, B. Schwartz, R. L. Keck, J. A. Delettrez, J. M. Soures, P. W. McKenty, V. N. Goncharov, J. P. Knauer, F. J. Marshall, D. D. Meyerhofer, P. B. Radha, S. P. Regan, T. C. Sangster, W. Seka, C. Stoeckl, "Capsule-areal-density asymmetries inferred from 14.7-MeV deuterium–helium protons in direct-drive OMEGA implosions", ***Phys. Plasmas*** 10, 1919 (2003).
49. R. D. Petrasso, J. A. Frenje, C. K. Li, F. H. Seguin, J. R. Rygg, B. E. Schwartz, S. Kurebayashi, P. B. Radha, C. Stoeckl, J.M. Soures, J. Delettrez, V.Yu. Glebov, D. D. Meyerhofer, T. C. Sangster, "Measuring Implosion Dynamics through rR Evolution in Inertial-Confinement Fusion Experiments", ***Phys. Rev. Lett.*** 90, 095002 (2003).
50. F. H. Seguin, J. A. Frenje, C. K. Li, D. G. Hicks, S. Kurebayashi, J. R. Rygg, B.-E. Schwartz, R. D. Petrasso, S. Roberts, J. M. Soures, D. D. Meyerhofer, T. C. Sangster, J. P. Knauer, C. Sorce, V. Yu. Glebov, C. Stoeckl, T. W. Phillips, R. J. Leeper, K. Fletcher, S. Padalino, **"**Spectrometry of charged particles from inertial-confinement-fusion plasmas", ***Rev. Sci. Instrum***. 74, 975 (2003).
51. T. C. Sangster, J. A. Delettrez, R. Epstein, V. Yu. Glebov, V. N. Goncharov, D. R. Harding, J. P. Knauer, R. L. Keck, J. D. Kilkenny, S. J. Loucks, L. D. Lund, R. L. McCrory, P. W. McKenty, F. J. Marshall, D. D. Meyerhofer, S. F. B. Morse, S. P. Regan, P. B. Radha, S. Roberts, W. Seka, S. Skupsky, V. A. Smalyuk, C. Sorce, J. M. Soures, C. Stoeckl, K. Thorp, J. A. Frenje, C. K. Li, R. D. Petrasso, F. H. Seguin, K. A. Fletcher, S. Padalino, C. Freeman, N. Izumi, J. A. Koch, R. A. Lerche, M. J. Moran, T. W. Phillips, G. J. Schmid, "Direct-drive cryogenic target implosion performance on OMEGA", ***Phys. Plasmas*** 10, 1937 (2003).
52. V. A. Smalyuk, J. A. Delettrez, S. B. Dumanis, V. Yu. Glebov, V. N. Goncharov, J. P. Knauer, F. J. Marshall, D. D. Meyerhofer, P. B. Radha, S. P. Regan, S. Roberts, T. C. Sangster, S. Skupsky, J. M. Soures, C. Stoeckl, R. P. J. Town, B. Yaakobi, J. A. Frenje, C. K. Li, R. D. Petrasso, F. H. Seguin, D. L. McCrorey, R. C. Mancini, J. A. Koch, "Hydrodynamic growth of shell modulations in the deceleration phase of spherical direct-drive implosions", ***Phys. Plasmas*** 10, 1861 (2003).
53. V. A. Smalyuk, P. B. Radha, J. A. Delettrez,V.Yu. Glebov,V. N. Goncharov, D. D. Meyerhofer, S. P. Regan, S. Roberts, T. C. Sangster, J.M. Soures, C. Stoeckl, J. A. Frenje, C. K. Li, R. D. Petrasso, F. H. Seguin, "Time-Resolved Areal-Density Measurements with Proton Spectroscopy in Spherical Implosions", ***Phys. Rev. Lett.*** 90, 135002 (2003).

V. GROUP CONFERENCE PRESENTATIONS DURING THE PERIOD OF THE GRANT

The following list includes talks by the MIT group and talks by our collaborators with MIT coauthors.

9th International Fast ignition workshop, Cambridge, MA (2006)

t1. R. D. Petrasso *et al*., "Monoenergetic particle backlighter for radiography and measuring E and B fields and plasma areal density".
t2. C. K. Li *et al.* "Measuring E and B fields with monoenegetic proton radiography".

48th APS Annual Meeting of the Division of Plasma Physics, (30 Oct. – 3 Nov. 2006, Philadelphia, PA)

t3. W. Theobald *et al.,* "High-Areal-Density, Fuel-Assembly Experiments for the Fast-Ignitor Concept," *Bull. Am. Phys. Soc.* 51, 31 (2006).
t4. P.B. Radha *et al.,* "Inferring Areal Density in OMEGA-DT Cryogenic Implosions," *Bull. Am. Phys. Soc.* 51, 106 (2006).
t5. J.A. Frenje *et al*., "Diagnosing Cryogenic D2 and DT Implosions at OMEGA using charged-particle spectrometry," *Bull. Am. Phys. Soc.* 51, 106-107 (2006).
t6. F.H. Seguin *et al*., "Using Target Shimming to Compensate for Asymmetric Drive in ICF Implosions," *Bull. Am. Phys. Soc.* 51, 107 (2006).
t7. G. Kyrala *et al*., "The Effect of High-z Impurities on Implosions and Burn in SIO2 Shells," *Bull. Am. Phys. Soc.* 51, 107-108 (2006).
t8. J. Benage *et al*., "Spectroscopic Measurements of ICF Capsules Doped with Hi-Z Impurities," *Bull. Am. Phys. Soc.* 51, 108 (2006).
t9. D.T. Casey *et al.,* "Diagnosing Cryogenic DT Implosions at OMEGA and the NIF using Magnetic Recoil Spectrometry (MRS)," *Bull. Am. Phys. Soc.* 51, 142 (2006).
t10. R.P.J. Town *et al*., "Proton Deflectometry of Electric and Magnetic Fields," *Bull. Am. Phys. Soc.* 51, 142 (2006).
t11. C.K. Li *et al*., "Measuring E and B Fields in Laser-Produced Plasmas through Monoenergetic Proton Radiography". *Bull. Am. Phys. Soc.* 51, 143 (2006).
t12. R.D. Petrasso *et al.,* "Monoenergetic Particle Backlighter for Radiography and Measuring E and B Fields and Plasma Areal Density". *Bull. Am. Phys. Soc.* 51, 143 (2006).
t13. N.D. Delamater *et al*., "Design of an Omega Experiment to Diagnose Ablator Burn-through with D-He3 Proton Yield and Spectra," *Bull. Am. Phys. Soc.* 51, 212-213 (2006).
t14. M. Manuel *et al.,* "Simulation of Monoenergetic Proton Radiography Images of ICF Hohlraums and Capsules," *Bull. Am. Phys. Soc.* 51, 218 (2006).
t15. G.A. Chandler *et al*., "CR39 Based Neutron Yield Measurements on the Z-Accelerator," *Bull. Am. Phys. Soc.* 51, 219 (2006).
t16. S.G. Glendinning *et al*., "Progress in Laser-Driven Dynamic Hohlraum Implosions," *Bull. Am. Phys. Soc.* 51, 265 (2006).
t17. D.D. Meyerhofer *et al.*, "Studies of Adiabat Shaping in Direct-Drive, Cryogenic-Target Implosions on OMEGA," *Bull. Am. Phys. Soc.* 51, 340 (2006).
t18. A. Miles *et al.,* "Numerical Simulations of thin-shell direct-drive OMEGA capsule implosions," *Bull. Am. Phys. Soc.* 51, 341 (2006).

16th High-temperature plasma diagnostics, (Invited) Williamsburg, Virginia (2006)

t19. C. K. Li *et al.,* "Monoenergetic proton backlighter for measuring E and B fields and for radiographing implosions and high-energy density plasmas".
t20. D. Casey *et al.,* "The Magnetic Recoil Spectrometer (MRS(Neutron Shielding and Collimator Design on OMEGA and the NIF".

36th Anomalous Absorption, Jackson Hole, Wyoming (2006)

t21. R. D. Petrasso *et al.,* "Monoenergetic particle backlighter for radiography and measuring E and B fields and plasma area density".
t22. C. K. Li *et al*. "Monoenergetic proton radiography of E and B fields".

47th APS Annual Meeting of the Division of Plasma Physics (24-28 Oct. 2005, Denver, CO)

t23. S.P. Regan *et al*., "Target Performance of Direct-Drive, D2-, D3He- and DT-filled, Plastic-Shell Implosions on OMEGA," *Bull. Am. Phys. Soc,* 50, 113 (2005).
t24. J.P. Knauer et al., "Direct Drive, Low-Adiabat ICF Implosions," *Bull. Am. Phys. Soc,* 50, (2005).
t25. T.C. Sangster *et al*., "Recent Cryogenic Implosion Results on Omega," *Bull. Am. Phys. Soc,* 50, 113-114 (2005).
t26. J.R. Rygg *et al*., "Studies of Shock Convergence in ICF Implosions Using Nuclear Burn History Measurements," *Bull. Am. Phys. Soc,* 50, 114 (2005).
t27. F.H. Seguin *et al*., "Measured Nuclear Burn Region Sizes and Symmetries in Direct-Drive ICF Implosions vs. Capsule and Drive Conditions," *Bull. Am. Phys. Soc,* 50, 114 (2005).
t28. S. Volkmer et al., "Improved Signal-to-Background Utilizing Coincidence Counting of Charged-Particle Tracks in CR-39," *Bull. Am. Phys. Soc,* 50, 116 (2005).
t29. M.J. Canavan *et al.,* "Characterization of a Fusion Product Source for ICF Diagnostic Development," *Bull. Am. Phys. Soc,* 50, 116-117 (2005).
t30. D.T. Casey *et al.,* "Shielding Design for the Magnetic Recoil Spectrometer (MRS) at OMEGA and the NIF using TART2002," *Bull. Am. Phys. Soc,* 50, 117 (2005).
t31. R.P.J. Town *et al*., "Calculating and Measuring Self-Generated Magnetic Fields in Hohlraums," *Bull. Am. Phys. Soc,* 50, 123-124 (2005).
t32. R.D. Petrasso *et al.,* "Energy Deposition, Penetration, Blooming of Energetic Electrons in Fast Ignition and Preheat Scenarios," *Bull. Am. Phys. Soc,* 50, 139 (2005).
t33. C.K. Li *et al.,* "Proton Radiography of Electromagnetic Fields Generated by Laser-Driven Plastic Foils," *Bull. Am. Phys. Soc,* 50, 266 (2005).
t34. J.A. Frenje *et al.,* "A Magnetic Recoil Spectrometer (MRS) for ρR, Yield and Tį Measurements of Implosions at OMEGA and the NIF," *Bull. Am. Phys. Soc,* 50, 267 (2005).
t35. C.D. Chen *et al.,* "Monte Carlo Simulations for Studying Hot-Electron Transport in Non-Degenerate Plasmas of Arbitrary Z," *Bull. Am. Phys. Soc,* 50, 293 (2005).

46th APS Annual Meeting of the Division of Plasma Physics (15-19 Nov. 2004, Savannah, GA)

t36. N.Izumi *et al*., "First Results of Implosion Experiments with OMEGA scale-3/4 Holraums," *Bull. Am. Phys. Soc,* 49, 26 (2004).
t37. P. Amendt *et al.,* "Measuring X-Ray Drive in Scale-3/4 Hohlraums Using the Proton Temporal Diagnostic (PTD): Design and Analysis," *Bull. Am. Phys. Soc,* 49, 26 (2004).
t38. T.C. Sangster *et al.,* "High-Areal-Density Cryogenic D2 Implosions on OMEGA," *Bull. Am. Phys. Soc,* 49, 61 (2004).
t39. S.P. Regan *et al.,* "Effects of the Low-*l*-Mode Irradiation Nonuniformities on the Performance of Direct-Drive Spherical Implosions," *Bull. Am. Phys. Soc,* 49, 62 (2004).
t40. J.A. Frenje *et al.,* "Measurements of Time Evolution of Ion Temperature of D3He Implosions on OMEGA," *Bull. Am. Phys. Soc,* 49, 63 (2004).
t41. J.R. Rygg *et a*l., "Inference of Imprint at Onset of Deceleration Phase Using Shock-Burn Measurements," *Bull. Am. Phys. Soc,* 49, 63 (2004).
t42. J.L. Ciantis *et al*., "Studying the Burn Region in ICF Implosions with Proton Emission Imaging," *Bull. Am. Phys. Soc,* 49, 63 (2004).
t43. F.H. Seguin *et al.,* "Relationship of Asymmetries in Fusion Burn and Areal Density to Asymmetries in Laser Drive for ICF Implosions at OMEGA," *Bull. Am. Phys. Soc,* 49, 63 (2004).

t44. C.K. Li *et a*l., "Linear-Energy Transfer and Blooming of Directed Energetic Electrons in Dense Hydrogenic Plasmas," *Bull. Am. Phys. Soc,* 49, 103 (2004).
t45. C.D. Chen *et al*., "Monte Carlo Simulations and Planned Experiments for Studying Hot-Electron Transport in H2 and D2," *Bull. Am. Phys. Soc,* 49, 103 (2004).
t46. J.M. Soures *et al*., "Polar-Direct-Drive Experiments on OMEGA," *Bull. Am. Phys. Soc,* 49, 180 (2004).
t47. D.C. Wilson *et al*., "Mixing in thick-walled and pulse-shaped directly driven ICF capsule implosions," *Bull. Am. Phys. Soc,* 49, 212 (2004).
t48. M. Canavan *et al*., "A Modified Accelerator for ICF Diagnostic Development," *Bull. Am. Phys. Soc,* 49, 238 (2004).

34th Annual Anomalous Absorption Conference (2 - 7 May 2004, Gleneden Beach, OR)

t49. J. DeCiantis *et al*., "Studying the Burn Region in ICF Implosions with Proton Emission Imaging".
t50. C. K. Li *et al*., "Effects of Nonuniform Illumination on Implosion Asymmetry in Direct-Drive Inertial Confinement Fusion".
t51. C. K. Li and R. D. Petrasso, "Stopping and Scattering of Directed Energetic Electrons in High-Temperature Hydrogenic Plasmas".
t52. J. A. Frenje, *et al*., "A High-Resolution Neutron Spectrometer for ρR_{fuel} and T_i Measurements at OMEGA and the NIF".
t53. J. R. Rygg *et al*., "An Empirical, Dynamic Mix Model for ICF Implosions".

15th Topical Conference on High Temperature Plasma Diagnostics (19 - 22 Apr. 2004, San Diego, CA)

t54. M. J. Canavan *et al*., "Diagnosing DT Cryogenic Fizzles at the NIF".
t55. J. DeCiantis *et al*., "Studying the Burn Region in ICF Implosions with Proton Emission Imaging".
t56. J. Frenje *et al*., "A Magnetic Recoil Spectrometer (MRS) for ρR_{fuel} and T_i Measurements of Warm, Fizzle and Ignited Implosions at the NIF".
t57. C. K. Li *et al*., "First Spectrometry of Charged Particles from Indirect-Drive Capsule Implosions".
t58. F.H. Séguin *et al*., "Proton Spectrometry and Imaging for Studying Performance and Dynamics of Inertial-Confinement-Fusion Experiments". (Invited talk)

DOE SSAA Symposium (29 – 31 March 2004, Albuquerque, NM)

t59. J. DeCiantis *et al*., "Studying the Burn Region in ICF Implosions with Proton Emission Imaging".
t60. C. K. Li *et al.*, "Effects of Nonuniform Illumination on Implosion Asymmetry in Direct-Drive Inertial Confinement Fusion".
t61. C. K. Li and R. D. Petrasso, "Stopping of Directed Energetic Electrons in High-Temperature Hydrogenic Plasmas".
t62. J. A. Frenje *et al*., "A high-resolution neutron spectrometer for ρR_{fuel} and T_i measurements at OMEGA and the NIF".
t63. J. R. Rygg *et al.,* "An Empirical, Dynamic Mix Model for ICF Implosions".

45th Annual Meeting of the Division of Plasma Physics (27 - 31 Oct. 2003, Albuquerque, NM)

t64. T. C. Sangster *et al*, "Experimental Results from Cryogenic D_2 Implosions on the OMEGA Laser," *Bull. Am. Phys. Soc.* 48, 55 (2003).

t65. V. Yu. Glebov *et al.,* "Secondary Neutron Energy Spectra Measurements with the 1020 Array on OMEGA," *Bull. Am. Phys. Soc.* 48, 55 (2003).
t66. F.J. Marshall *et al.,* "Direct-Drive Implosions on OMEGA with Optimized Illumination Uniformity," *Bull. Am. Phys. Soc.* 48, 56 (2003).
t67. J. R. Rygg *et al*., "Experimental Studies of Time-Dependent Mix in OMEGA Direct-Drive Implosions," *Bull. Am. Phys. Soc.* 48, 57(2003).
t68. F. H. Seguin *et al*., "Direct Measurement of ρR-Asymmetry Time Evolution in OMEGA Implosions," *Bull. Am. Phys. Soc.* 48, 57 (2003).
t69. C. K. Li *et al*., "Using Charged Particles to Measure ρR and ρR Asymmetries for Indirect-Drive Implosions," *Bull. Am. Phys. Soc.* 48, 57 (2003).
t70. J. R. Rygg et al., "The effects of implosion asymmetry on shock convergence in OMEGA experiments," *Bull. Am. Phys. Soc.* 48, 57-58 (2003).
t71. S. Kurebayashi *et al*., "Investigation of the Use of Secondary Protons and Neutrons for Studying Fuel Areal Density in imploded, D_2-Filled Inertial Capsules," *Am. Phys. Soc.* 48, (2003).
t72. J. DeCiantis *et al.,* "Studying the burn regions in ICF implosions with Proton Emission Imaging,"
t73. *Bull. Am. Phys. Soc.* 48, 58 (2003).
t74. J. P. Knauer *et al*, "Direct-Drive ICF Implosions with Picket-Fence Pulse Shapes," *Bull. Am. Phys. Soc.* 48, 255 (2003).
t75. J. A. Frenje *et al*., "A Magnetic Recoil Spectrometer (MRS) for Precise ρR_{fuel} and T_i Measurements of Warm, Fizzle and Ignited Implosions at OMEGA and the NIF," *Bull. Am. Phys. Soc.* 48, 287 (2003).
t76. M. J. Canavan et al., "The utility of knock-on D, T, and P for diagnosing NIF implosions," *Bull. Am. Phys. Soc.* 48, 320 (2003).
t77. V. Yu. Glebov *et al*, "Proton Temporal Diagnostic for ICF Experiments on OMEGA," *Bull. Am. Phys. Soc.* 48, 342 (2003).

3rd International Conference on Inertial Fusion Sciences and Applications (7 - 12 Sept. 2003, Monterey, CA)

t78. C. K. Li et al., "ρR Asymmetry in Spherical Implosions of Inertial Confinement Fusion".
t79. J. A. Frenje et al., "Measurements of Shock-Coalescence Timing of D^3He Implosions at OMEGA".
t80. J. A. Frenje et al., "A Novel Magnetic Recoil Spectrometer (MRS) for Precise ρR_{fuel} and T_i Measurements of Warm and Cryo OMEGA Implosions, and Warm, Fizzle and Ignited NIF Implosions".
t81. P. W. McKenty et al., "Direct-Drive Cryogenic Target Implosion Performance on OMEGA".

33rd Annual Anomalous Absorption Conference (22 - 27 June 2003, Lake Placid, NY)

t82. C. K. Li *et al*., "Using Charged Particles to Measure ρR and ρR Asymmetries for Indirect-Drive Implosions".
t83. J. A. Frenje *et al*., "Measurement of Shock-Coalescence Timing and ρR Evolution of D^3He Implosions at OMEGA".
t84. J. A. Frenje *et al*., "A Magnetic Recoil Spectrometer (MRS) for Precise ρR_{fuel} and T_i Measurements of Warm and Cryo Targets at OMEGA and the NIF".
t85. F. H. Seguin *et al.,* "Time Evolution of ρR Asymmetries in OMEGA Direct-Drive Implosions".
t86. R. Rygg *et al*., "The Effects of Implosion Asymmetry on Shock Coalescence in OMEGA Experiments".
t87. S. Kurebayashi *et al.,* "Using Secondary Protons and Neutrons to Study ρR_{fuel}".
t88. J. DeCiantis *et al*., "Imaging DD and D^3He Burn Profiles on OMEGA Implosions".

VI. REFERENCES

The following list of references includes many papers written by the MIT group; for more, see http://psfcwww2.psfc.mit.edu/physics_research/hedp/Papers/Papers.html). Black entries are by MIT as either first authors or co-authors. Blue entries are by other authors.

1. J. D. Lindl, Inertial Confinement Fusion (Springer-Verlag, New York, 1999).
2. S. W. Haan *et al.*, *Phys. Plasmas* **2**, 2480 (1995).
3. D. D. Meyerhofer *et al.*, *Phys. Plasmas* **8** (5), 2251 (2001).
4. D. D. Meyerhofer *et al.*, *Plasma Phys. Contr. Fusion* **43**, A277 (2001).
5. R. D. Petrasso *et al.*, *Phys. Rev. Lett.* **77** (13), 2718 (1996).
6. C. K. Li *et al.*, *Phys. Rev. Lett.* **70** (20), 3059 (1993).
7. C. K. Li *et al.*, *Phys. Rev. Lett.* **70** (20), 3063 (1993).
8. F. H. Seguin *et al.*, *Rev. Sci. Instrum.* **74**, 975 (2003).
9. F. H. Séguin *et al.*, *Phys. Plasmas* **9**, 2725 (2002).
10. F. H. Séguin *et al.*, *Phys. Plasmas* **9**, 3558 (2002).
11. F. H. Séguin, Bull. Am. Phys. Soc. **47** (2002).
12. C. K. Li *et al.*, *Phys. Rev. Lett.* **92**, 205001 (2004).
13. F. H. Séguin *et al.*, Bull. Am. Phys. Soc. **48**, 57 (2003).
14. J. A. Frenje *et al.*, *Phys. Plasmas* **11**, 2798 (2004).
15. R. D. Petrasso *et al.*, *Phys. Rev. Lett.* **90**, 095002 (2003).
16. P. W. McKenty *et al.*, *Phys. Plasmas* **11**, 2790 (2004).
17. T. C. Sangster *et al.*, *Bull. Am. Phys. Soc*. **49**, 61 (2004).
18. J. D. Lindl *et al.*, *Phys. Plasmas* **11**, 339 (2004).
19. P. A. Amendt *et al.*, *Bull. Am. Phys. Soc*. **49**, 26 (2004).
20. N. Izumi *et al.*, *Bull. Am. Phys. Soc*. **49**, 26 (2004).
21. F. H. Séguin *et al.*, *Rev. Sci. Instrum.* **75**, 3520 (2004).
22. F. H. Seguin *et al.*, *Phys. Plasmas* **13**, 082704 (2006)
23. F. H. Seguin *et al.*, "Target shimming for control of ICF implosion symmetry", in preparation for submission (2007).
24. C. K. Li *et al.*, *Phys. Rev. Lett.* **89**, 165002 (2002).
25. J. L. DeCiantis *et al.*, *Rev. Sci. Instrum*. **77**, 043503 (2006).
26. D.A. Callahan *et al.*, Nucl. Inst. Methods A **544**, 9 (2005).
27. S. Skupsky *et al.*, Phys. Plasmas **11**, 2763 (2004).
28. C. K. Li *et al.*, *Rev. Sci. Instrum.* **77**, 10E725 (2006).
29. C. K. Li *et al.*, *Phys. Rev. Lett.* **97** 135003 (2006).
30. C. K. Li *et al.*, "Observation of the Decay Dynamics and Instabilities of Megagauss Magnetic Field Structures in Laser-Produced Plasmas", accepted for publication in *Phys. Rev. Lett.* (2007).
31. C. K. Li *et al.*, "Observation of Megagauss Field Topology Changes due to Magnetic Reconnection in Laser-Produced Plasmas", submitted to *Phys. Rev. Lett* (2007).
32. J.R. Rygg *et al.*, "Dual nuclear product observations of shock collapse in inertial confinement fusion", submitted to *Phys. Rev. Lett.* (2007).
33. J. R. Rygg *et al.*, *Phys. Plasmas* **14**, 056306 (2007).
34. D. C. Wilson *et al.*, *Phys. Plasmas* **11**, 2723 (2004).
35. J. R. Rygg *et al.*, "Dual nuclear product observations of shock collapse in inertial confinement fusion", submitted to *Phys. Rev. Lett.* (2007).
36. F. H. Séguin *et al.*, *Bull. Am. Phys. Soc*. **49**, 63 (2004).
37. D. G. Hicks *et al.*, *Rev. Sci. Instrum.* **68**, 589 (1997).
38. K. W. Wenzel *et al.*, *Rev. Sci. Instrum.* **63**, 4837 (1992).
39. J. A. Frenje *et al.*, *Rev. Sci. Instrum*. **72**, 854 (2001).
40. J. A. Frenje *et al.*, Proposal #DE-FG03-03NAS00058.

41. J.A. Frenje *et al.*, "A magnetic recoil spectrometer (MRS) for absolute measurements of the neutron spectrum from which ρR, Ti and yield can be inferred for cryogenic DT implosions at OMEGA and the NIF", in preparation for submission (2007).
42. D.T. Casey *et al.*, "Background characterization and reduction for the Magnetic Recoil Spectrometer (MRS) at OMEGA and the NIF", in preparation for submission (2007).
43. C. Stoeckl *et al., Rev. Sci. Instrum.* **74**, 1713 (2003).
44. C. K. Li *et al., Phys. Plasmas* **7**, 2578 (2000).
45. P. B. Radha *et al.*, *Phys. Plasmas* **9**, 2208 (2002).
46. Tabak, LLNL patent, 1997.
47. Norreys *et al.*, *Phys. Plasmas* **7**, 3721 (2000).
48. M. H. Key *et al*., *Phys. Plasmas* **5**,1966 (1998).
49. M. Tabak *et al.*, *Phys. Plasmas* **1**, 1626 (1994).
50. C. Stoeckl *et al., Plasma Phys. Control. Fusion* **47**, B859 (2005).
51. C. K. Li *et al.*, *Phys. Rev.* E **70**, 067401 (2004).
52. C. K. Li *et al.*, *Phys. Rev.* E **73**, 016402 (2006).
53. J. Delettrez *et al.*, *Bull. Am. Phys. Soc*. **49**, 103 (2004).

APPENDIX a: STATEMENT OF WORK for Nuclear Probing of Dense Plasmas (2002)

A. ρR symmetry measurements at burn time

i. Direct-drive ρR symmetry measurements

1. Study correlations of measured ρR asymmetries with purposely-introduced asymmetries in laser energy deposition (particularly the $\ell = 1$ mode).
2. Study correlation of measured ρR asymmetries with other data relevant to asymmetry (*e.g.* x-rays).

ii. Indirect-drive ρR symmetry measurements

3. Study correlations of measured ρR asymmetries with different laser-pointing configurations.
4. Study correlations of measured ρR asymmetries with different capsule parameters.

B. Proton-Core-Imaging Spectroscopy of the D(^{3}He, α)p burn profile

1. Perform experiments to determine optimal imaging-system parameters.
2. Design and fabricate a proton camera, based on the optimal parameters determined as above.
3. Measure radial burn profiles from a single camera.
4. Study burn asymmetries using a single camera by deconvolving 2-dimensional image content.

C. The slowing down of charged particles in dense plasmas

1. Measure the energy loss of up to six different products from D-T-^{3}He capsules at OMEGA; compare to theory.
2. Explore the feasibility of experiments to test regimes of stopping power theory in which either the electron or ion component dominates.
3. Design and attempt particle-slowing-down experiments proposed by N. Hoffman of LANL.

D. Fuel-shell mix in capsule implosions

i. Direct-drive experiments

1. Extend implosion experiments of CD sub-layered capsules filled with pure ^{3}He gas to study how fuel-shell mix is correlated with capsule parameters.
2. Extend implosion experiments of ICF-relevant plastic capsules filled with D_2 or D-T gas to study the correlation between mix and target performance and to benchmark code predictions.
3. Apply mix models to data from tasks D-1 and D-2; study the physical processes involved in mix.

ii. Indirect-drive experiments

4. Investigate the feasibility of implementing charged-particle spectroscopy to study fuel-shell mix.

E. ρR determination at shock-coalescence time and at bang time

1. Measure proton spectra from implosions of D-^{3}He filled capsules with various shell thicknesses to assess differences in ρR at shock and bang time.
2. At shock time, measure temperatures and yields.
3. Study asymmetry at shock and bang times to see if such asymmetries are amplified or diminished.
4. Measure differences in size, if discernable, between the compression and shock burn regions.
5. Compare these results to analytic and code predictions to elucidate the basic implosion physics.
6. Attempt to study fuel-shell mix at shock-coalescence and bang times.

F. Upgrading diagnostics

i. New methods for scanning and analyzing CR-39

1. Upgrade the hardware used for extracting data from CR-39 track detectors.
2. Upgrade the software used for controlling the data acquisition process.
3. Upgrade the software used for analyzing data.
4. Characterize thin CR-39 for use in proton imaging cameras.

ii. New Wedge-Range-Filter (WRF) spectrometers

5. Make new Wedge-Range-Filter spectrometers for indirect-drive experiments.

6. Make new Wedge-Range-Filter spectrometers for symmetry studies in direct-drive experiments.

G. Upgrading the MIT 170-kV Cockcroft-Walton accelerator for developing, testing, and calibrating ICF diagnostics, and for training students

1. Replace the accelerator tube.
2. Design and fabricate a new target chamber suitable for the calibration studies of new ICF diagnostics that are described in Sec. 3G.
3. Design and fabricate a new target holder enabling target changes without breaking vacuum.

H. Education

1. Recruit students at graduate and undergraduate levels.
2. Stimulate students with challenging problems in ICF, nuclear physics and astrophysics.
3. Give students hands-on experience with nuclear techniques and methodologies using small-scale experiments.
4. Give students experience working with big collaborations and large experiments such as OMEGA and the NIF.

APPENDIX b: STATEMENT OF WORK for Purchase of the Magnet for a Magnetic-Recoil Spectrometer (2003)

The one task to be funded [by this proposal] is the purchase of the magnet required for the Magnetic Recoil Spectrometer for neutron spectrometry of the NIF. The magnet design, described in [the proposal], has been approved at the Conceptual Design Review (CDR) held at the Laboratory for Laser Energetics (LLE) on 17 April 2003. The CDR involved personnel from MIT, LLE, and LLNL.